EUR 4875 e

COMMISSION OF THE EUROPEAN COMMUNITIES

European Atomic Energy Community - EURATOM
FIAT S.p.A., Sezione Energia Nucleare - Torino
Società ANSALDO S.p.A. - Genova

FORCED CONVECTION BURNOUT AND HYDRODYNAMIC INSTABILITY EXPERIMENTS FOR WATER AT HIGH PRESSURE

Part VIII: Analysis of burnout experiments on 3x3 rod bundles with uniform and non-uniform heat generation

by

E. di CAPUA and R. RICCARDI
(FIAT)

1972

Contract No. 008-61-12 PNII

LEGAL NOTICE

This report is on sale at the addresses listed on cover page 4

at the price of B.Fr. 100,–

Commission of the
European Communities
D.G. XIII - C.I.D.
29, rue Aldringen
L u x e m b o u r g

November 1972

4875 e

FORCED CONVECTION BURNOUT AND HYDRODYNAMIC INSTABILITY EXPERIMENTS FOR WATER AT HIGH PRESSURE
Part VIII: Analysis of burnout experiments on 3×3 rod bundles with uniform and non-uniform heat generation
by E. di CAPUA and R. RICCARDI (Fiat)

European Atomic Energy Community - EURATOM
FIAT S.p.A., Sezione Energia Nucleare - Torino
Società ANSALDO S.p.A. - Genova
Contract No. 008-61-12 PNII
Luxembourg, November 1972 - 76 Pages - 23 Figures - B.Fr. 100.—

The analysis of burnout tests in a 3×3 rod bundle is performed, including tests with uniform and non-uniform axial and transversal heat generation.

The calculation method used in this analysis is the introduction of local parameters calculated by an openchannel thermohydraulic code in some Critical Heat Flux correlations choosen for their wide validity range. More than 240 experimental tests are analyzed in this report, and the results appear to be fully satisfactory, giving a maximum approximation of 25%.

4875 e

FORCED CONVECTION BURNOUT AND HYDRODYNAMIC INSTABILITY EXPERIMENTS FOR WATER AT HIGH PRESSURE
Part VIII: Analysis of burnout experiments on 3×3 rod bundles with uniform and non-uniform heat generation
by E. di CAPUA and R. RICCARDI (Fiat)

European Atomic Energy Community - EURATOM
FIAT S.p.A., Sezione Energia Nucleare - Torino
Società ANSALDO S.p.A. - Genova
Contract No. 008-61-12 PNII
Luxembourg, November 1972 - 76 Pages - 23 Figures - B.Fr. 100.—

The analysis of burnout tests in a 3×3 rod bundle is performed, including tests with uniform and non-uniform axial and transversal heat generation.

The calculation method used in this analysis is the introduction of local parameters calculated by an openchannel thermohydraulic code in some Critical Heat Flux correlations choosen for their wide validity range. More than 240 experimental tests are analyzed in this report, and the results appear to be fully satisfactory, giving a maximum approximation of 25%.

4875 e

FORCED CONVECTION BURNOUT AND HYDRODYNAMIC INSTABILITY EXPERIMENTS FOR WATER AT HIGH PRESSURE
Part VIII: Analysis of burnout experiments on 3×3 rod bundles with uniform and non-uniform heat generation
by E. di CAPUA and R. RICCARDI (Fiat)

European Atomic Energy Community - EURATOM
FIAT S.p.A., Sezione Energia Nucleare - Torino
Società ANSALDO S.p.A. - Genova
Contract No. 008-61-12 PNII
Luxembourg, November 1972 - 76 Pages - 23 Figures - B.Fr. 100.—

The analysis of burnout tests in a 3×3 rod bundle is performed, including tests with uniform and non-uniform axial and transversal heat generation.

The calculation method used in this analysis is the introduction of local parameters calculated by an openchannel thermohydraulic code in some Critical Heat Flux correlations choosen for their wide validity range. More than 240 experimental tests are analyzed in this report, and the results appear to be fully satisfactory, giving a maximum approximation of 25%.

EUR 4875 e

COMMISSION OF THE EUROPEAN COMMUNITIES

European Atomic Energy Community - EURATOM
FIAT S.p.A., Sezione Energia Nucleare - Torino
Società ANSALDO S.p.A. - Genova

FORCED CONVECTION BURNOUT AND HYDRODYNAMIC INSTABILITY EXPERIMENTS FOR WATER AT HIGH PRESSURE

Part VIII: Analysis of burnout experiments on 3x3 rod bundles with uniform and non-uniform heat generation

by

E. di CAPUA and R. RICCARDI
(FIAT)

1972

Contract No. 008-61-12 PNII

ABSTRACT

The analysis of burnout tests in a 3×3 rod bundle is performed, including tests with uniform and non-uniform axial and transversal heat generation.

The calculation method used in this analysis is the introduction of local parameters calculated by an openchannel thermohydraulic code in some Critical Heat Flux correlations choosen for their wide validity range. More than 240 experimental tests are analyzed in this report, and the results appear to be fully satisfactory, giving a maximum approximation of 25%.

KEYWORDS

PWR TYPE REACTORS	CORRELATIONS
FUEL ELEMENT CLUSTERS	ANALYTICAL SOLUTION
FORCED CONVECTION	COMPUTER CALCULATIONS
BURNOUT	MEASURED VALUES
CRITICAL HEAT FLUX	RELIABILITY

NOTICE

Under the Euratom/Fiat-Ansaldo contract of association for the development of a pressurized water marine reactor a series of experiments on burnout phenomena were carried out. The results of this programme were published in the final report :
EUR 4630i "Nave Cisterna a propulsione nucleare - Rapporto Finale "
as well as in seven of the "topical reports" which together form Part 2 of Vol. II of this final report.

After the expiration of the contract, additional experiments were conducted by the SORIN Heat Transfer Laboratory and the Heat Transfer Laboratory of the Euratom Joint Research Centre at Ispra in an attempt to supplement the data obtained. The results of these experiments are described in the present report.

Topical Reports on FORCED CONVECTION BURNOUT AND HYDRODYNAMIC INSTABILITY EXPERIMENTS FOR WATER AT HIGH PRESSURE already published :

EUR 2490e - Part I: (Full-size)	Presentation of Data for Round Tubes with Uniform and Non-uniform Power Disbribution (1965).
EUR 2963e - Part II : (Full-size)	Presentation of Data for Water Flowing Upward Along a Uniformly Heated Rod in a Square Unheated Duct (1966).
EUR 3113e - Part III: (Full-size)	Comparison Between Experimental Burnout Data and Theoretical Prediction for Uniform and Non-uniform Heat Flux Distribution (1966).
EUR 3881e - Part IV: (Full-size)	Burnout Experiments in a Double Channel Test Section with Transversely Varying Heat Generation (1968).
EUR 4070e - Part V: (Full-size)	Analysis of Heating and Burnout Experiments in a Double Channel Test Section with Transversely Varying Heat Generation (1968).
EUR 4468e - Part VI: (Full-size)	Burnout Heat Flux Measurements on 9 Rod Bundles with Longitudinally and Transversally Uniform Heat Generation (1970).
EUR 4514e - Part VII: (Full-size)	Burnout heat flux measurements on 3 x 3 rod bundles with non-uniform heat generation (1970).

I N D E X

LIST OF TABLES

LIST OF FIGURES

./.

INTRODUCTION

An important factor in the design and development of water-cooled reactor cores is the maximum heat transfer rate or critical heat flux (CHF) at which fuel elements can be safely operated.

In pressurized water reactors the fuel elements are in form of rod bundles, and the prediction of the CHF presents problems such as mixing between subchannels, determination of local parameters along single channels, and application of traditional CHF correlations.

The finality of the present work is to compare the experimental data obtained in a 3 x 3 rod bundle with the predictions of correlations, which use the local parameters calculated by an open-channel thermohydraulic code.

The experimental data have been obtained from a research program performed under a contract between Euratom, Fiat and Ansaldo with the participation of CNEN.

The experiments have been carried out by SORIN Heat Transfer Laboratory and Heat Transfer Laboratory of the ISPRA C.C.R. EURATOM.

The data cover uniform and non-uniform power distribution and cold-wall effects in a series of rod combinations which simulate real situations in a PWR core.

CH. 1 - CRITICAL HEAT FLUX ANALYSIS PROCEDURE

The procedure used for the analysis of the DNB tests, reported in Ref. 6 and 7 , and described in Ch. 2, can be schematized as follows.

First, a subchannel analysis of the assembly is performed, with a division of the assembly into a certain number of adjacent channels and of axial increments of equal length.

Exchanges of mass, energy and momentum between adjacent channels are allowed.

Local density, mass velocity, enthalpy, steam quality, pressure drop are thus evaluated for each channel and each length step. The details of this analysis, which is performed by a computer code named MICRO-3, are presented in Appendix A.

The above mentioned local parameters are then used for the evaluation of DNBRs according to some Critical Heat Flux correlations, which are presented hereafter.

We have done a preliminary analysis of the existing CHF correlations, in order to choose the most reliable to an open-channel point of view of the problem.

One of the main problems is the corner cells situation, with the unheated walls and the unheated rods which are introduced in some of the experiments we examined.
Some correlations have "unheated wall" or "cold wall" corrections, and they were used in MICRO-3, together with others prepared by FIAT.

We give hereafter a list of the correlations with their validity range.

- W-3 correlation (Ref. 1).

Form:

$$\frac{q''_{DNB}}{10^6} = \left[(2,02 - 0,43\ p/_{10^3}) + (0,172 - 0,1\ p/_{10^3}) \cdot \right.$$
$$\left. \cdot \exp\,(18,2\ x - 4,13\ x\ p/_{10^3})\right] \cdot \left[1,16 - 0,87\ x\right] \cdot$$
$$\cdot \left[(0,148 - 1,6\ .x + 0,173\ x|x|) .\ G/_{10^6} + 1,04\right] \cdot$$
$$\cdot \left[0,266 + 0,836\ \exp\,(- 3,15\ De)\right] \cdot \left[0,826 + \right.$$
$$\left. + 0,0008\ (H_{sat} - H_{in})\right] ;$$

H_{in} and H_{sat} are inlet and saturation enthalpies.

Validity range:

- Pressure p	1000 - 2300 psia	70 - 162 kg/cm^2
- Mass flow rate G	1-5 . 10^6 $lb/hr.ft^2$	135-675 gr/cm^2 sec
- Hydraulic diameter D_e	0.2 - 0.7 in.	5,1 - 17,8 mm.
- Outlet quality X_{ex}	$\leqslant 0.15$	
- Heated length L	10 - 144 in.	254 - 3657 mm.

- ΔH FIAT correlation (Ref. 2).

Form:

$$\frac{\Delta H_{DNB}}{H_{fg}} = 0,84848 \cdot \alpha \cdot \frac{(H_{sat} - H_{in})}{H_{fg}} + 0,153945 \; (0,45 -$$

$$- 0,3 \; \frac{p - p_o)}{10^3} \cdot \left(\frac{G}{10^6}\right)^{-0,874} + 0,119932 \; L^{0,5} +$$

$$+ 1,088892 \; (e^{-8,13 \; De^{0,85}}) + 0,067711 \; \left(\frac{G}{10^6}\right)^{-0,874}$$

$$(\rho_g / \rho_f)^{-0,533} - 0,89265 \; ;$$

where $\alpha = \left[1 - 3 \left(\frac{G}{10^6} - 1,1\right) \cdot 10^{-4} \; (2000 - p)\right] \frac{L^{0,3}}{De^{0,5}}$

and $p_o = 1000$ psia

H_{sat}, H_{in} and H_{fg} are saturation, inlet and evaporation en-thalpies.

ρ_f and ρ_g are saturation liquid and gas densities.

./.

Validity range:

- Pressure p	1000 - 2000 psia	70 - 140 kg/cm^2
- Mass flow rate G	0,35-2,5$\cdot 10^6$ lb/hrft^2	47,5-340 gr/cm^2$\cdot$sec
- Hydraulic diameter D_e	0,22-1,475 in.	5,6-37,5 mm
- Outlet quality X_{ex}	>0	
- Heated length L	17-79 in.	432 - 2000 mm

- GE correlation (Ref. 3 and 4)

Form:

$$\frac{q''DNB}{10^6} = \frac{\left[1 + 0{,}16 \left(\frac{1000-p}{400}\right)^2 - 0{,}04 \left(\frac{1000-p}{400}\right)^2\right]}{1 - 0{,}008\ E\ (G/10^6)^{+0{,}8}} \left\{0{,}0172\ E\left(\frac{G}{10^6}\right)^{0{,}8} -\right.$$

$$- \left[0{,}3175 \left(\frac{G}{10^6}\right)^{-2} - 1{,}85 \left(\frac{G}{10^6}\right)^{-1}\right] - \left[2{,}4 + 3{,}2\ De + 0{,}83\right.$$

$$\left. De \left(\frac{G}{10^6}\right)\right] \cdot \left[x - 0{,}0629 \left(\frac{G}{10^6}\right)^{-2} + 0{,}343 \left(\frac{G}{10^6}\right)^{-1} - 0{,}249 +\right.$$

$$\left.\left. + 0{,}002 \left(\frac{G}{10^6}\right)^2\right]\right\} \quad ;$$

where $E = (D_o/D_i)^{0.5}\ (D_o - D_i)^{-0.2}$

This correlation has been prepared for annulus clusters. Consequently it is not reliable to central and wall channels. D_o and D_i are outer and inner diameter of the cluster.

Validity range:

- Pressure p	600 - 1450 psia	42 - 102 kg/cm^2
- Mass flow rate G	0,2-6,2$\cdot 10^6$ lb/hr ft^2	27-840 gr/cm^{2}sec
- Hydraulic diameter D_e	0,25 - 0,875 in.	6,35 - 22,2 mm
- Outlet quality X_{ex}	- 0,12 - +0,44	
- Heated length L	$\leqslant$108 in.	$\leqslant$2743,2 mm

Our test section is provided with unheated walls and unhea ted rods, and CHF correlations require a cold wall correction in the subchannels which are in this situation. We used a cold wall factor given by Tong et al. (Ref. 5).

$$\frac{q"DNB}{q\,hDNB} = (1,36 + 0,2e^{9x})(1,2 - 1,6e^{-1,922P_h}).(1,33 - 0,237e^{5.66x})$$

which has the same validity range of W-3 correlation.
P_h is the heated perimeter.

This formulation did not give good results (see fig. 2). We have then used cold wall corrections, prepared for both W-3 and ΔH FIAT correlations, which take in account a greater number of parameters, such as hydraulic and heated diameters ratio, mass flow rate, quality and pressure. The validity range is the same of W-3 correlation, with the exception of quality, which is positive for ΔHFIAT. For its peculiar origin, we have applied GE correlation only to "corner cells", which may recall a quarter of an annulus. Naturally, the correlations which allow a complete analysis in the cluster are W-3 for subcooled DNB and ΔHFIAT for quality DNB region, owing to their "cold-wall" correction. MICRO-3 computer program calculates DNB ratio also for W-3 correlation with the upmentioned Tong's correction and for W-2 correlation with cold-wall correction; we are not going to comment these results, due to the fact that the W-2 correlation we used was declared absolete by its authors.

CH. 2 - EXPERIMENTAL PROGRAM DESCRIPTION

The experiments upon which the analysis has been based are reported in Ref. 6 and 7 . We report hereafter a brief description of them.
The program is also summarized in figure 1.

The tests can be subdivided in the following two groups:

a) Uniform tests, which are tests with uniform heat generation, both in the axial and transversal direction, and with uniform subchannel geometrical configuration (grids, rod diameter).
Two different 3 x 3 test sections have beed used, differing in the distance of the shroud wall from the rods: a first configuration in which this distance is equal to the half-pitch (half of the distance between two rods) so that the flow area of a corner and lateral subchannel is equal to the flow area of a central channel; a second configuration with an "extragap", in which the distance of the shroud wall from the rod is equal to the half-pitch plus 1,06 mm. The first configuration is relative to Channel A - Set 0 in Figure 1; the second configuration to Channel B - Set 0.
The presence of an extra-gap has a strong influence on the cold wall effect.
The parameter range covered by these tests is:

- Pressure	1195 - 2247 psia	84 ÷ 158 Kg/cm^2
- Mass flow rate	$0{,}37-2{,}212 \cdot 10^6$ $lb/hrft^2$	50÷300 $gr/cm^2 \cdot sec$
- Inlet temperature	317 - 547 °F	194 ÷ 322 °C
- Exit quality	-0,34 ÷ +0,53	

b) Non-uniform tests, that is tests with non uniform heat generation both in axial and transversal direction, and/or with non uniform subchannel geometrical configurations (grids, rod diameter).
All these tests have been performed with the "extragap" shroud configuration (Channel B).
In the non uniform tests, a series of different configuration has been prepared, in order to simulate various situations existing in a reactor core:

Set I. Experiments in a 9 rod bundle uniformly heated both in longitudinal and transversal directions, characterized by ostructions in the flow area of some subchannels.

Set II. Experiments in a 9 rod bundle characterized by singularities in the transversal heat generation across the bundle, the longitudinal heating being uniform. These tests are further subdivided in the following way:

Set II.1. Experiments in a 9 rod bundle with the central rod unheated and of larger diameter in order to simulate the guide tube of a "Cluster Control" element.

Set II.2. Experiments in a 9 rod bundle with 3 side rods unheated and with the same outer diameter as the heated ones.

Set II.3. Experiments in a 9 rod bundle with the 4 corner rods unheated and with the same outer diameter as the 5 heated ones (the power of 3 rods has been overloaded by a factor of 23%).

Set II.4. Experiments in a 9 rod bundle with the 4 corner rods unheated, one simulating the "Cluster Control" guide tube and the remaining rods with the same outer diameter as the 5 heated ones (three of these 23% overloaded).

Set II.5. Experiments in a 9 rod bundle in which the three rows of rods ware heated at different power levels.

Set III. Experiments in a 9 rod bundle having the 4 corner rods unheated, a rod of larger diameter simulating the "Cluster Control" guide tube and the remaining rods heated with a non-uniform longitudinal power distribution.

The parameter range covered by the experiments is:

- Pressure	611 - 2247 psia	43 ÷ 158 kg/cm^2
- Mass flow rate	$0{,}34-2{,}27 \cdot 10^6$ $lb/hrft^2$	47÷308 $gr/cm^2 sec$
- Inlet temp.	281 - 558 °F	174 ÷ 328 °C

Further informations can be found in the original reports, describing the experimental tests (Ref. 6 , and Ref. 7).

CH. 3 - DESCRIPTION OF THE ANALYSIS

Using the input data given by the mentioned reports we have performed 250 tests of MICRO-3 program, in order to have the elements for a valid comparison between experimental DNB data and theoretical predictions.

The results are presented by means of tables and diagrams, following the same order of the experimental program.

The values of DNBR reported are to be considered the lowest among the DNBRs of the various subchannels surrounding the rod in which DNB signal has experimentally been detected. The local quality is referred to that particular subchannel. If the subchannel contains a cold wall, the program gives the prediction with cold wall correction.
For the precision in the indication of DNB position (i.e. the minimum DNB ratio is located in a subchannel surrounding the experimental DNB rod) we report hereafter the percentage of success in each group of tests.

Channel	A.	Set.	O.	(36	tests	analyzed)	100%
"	B.	"	O.	(58	"	")	69%
"	B.	"	I.	(10	"	")	70%
"	B.	"	II.1	(19	"	")	100%
"	B.	"	II.2	(16	"	")	80%
"	B.	"	II.3	(18	"	")	100%
"	B.	"	II.4	(18	"	")	61%
"	B.	"	II.5	(18	"	")	56%
"	B.	"	III.	(55	"	")	100%

In the next pages we review the results of each set of experiments singularly analyzed with the ΔH-FIAT and W-3 predictions; a short comment on the use of the General Electric correlation for corner subchannels will follow. The subchannel subdivision we have used is presented in Appendix B, where examples of the complete main outputs of MICRO-3 are shown also for each set of experimental tests.

UNIFORM TESTS

Channel A - Set 0.
Channel B - Set 0.
(tables I and II, fig. 3, 4, 5, 6)

Experimentally we have always DNB on the corner rod for channel A tests. The fact is due to the cold wall which is near the corner rod.
The experiments were held at fairly high qualities, so we have a good number of ΔH-FIAT predictions.
Depending on the pressure range, the correlation gives values of DNBR going from 0,8 to 1,0.
The greatest accuracy of prediction is obtained for DNB qualities going up to 20-25%. Incidentally we observe that this is the quality for which the lowest theoretical DNBR goes from the corner cell to the central one.
As for W-3 correlation predictions we had not many results due to the high qualities of the experimental tests. The predictions are good, going from 0,9 to 1,2 with only one exception. DNB is predicted to be always in the central channel, as we can very well see in Table I in which the DNB quality predicted for the central channel is often different from the quality in the corner channel (ΔH-FIAT prediction).
Always regarding set A, we must say that, owing naturally to the little gap between shroud wall and rods, the MICRO-3 program predicts strong mass flow rate redistributions in the peripherical channels (e.g. in the corner channel the outlet mass flow rate is, in average, 0,77 times the inlet mass flow rate).

In channel B tests the extra-gap at the wall cells brings two main differences from channel A tests:

1) there is a smaller cold-wall penalty, due to the larger corner gap;
2) the mass flow rate redistribution among the subchannels is also smaller.

Experimentally, DNB occurs no more exclusively on the corner rod, but also on side rods and on the central one.

In this set we have the greatest part of the experiments held at high qualities. ΔH-FIAT gives DNBR values going from 0,85 to 1,1. Moreover for this set greater accuracy of prediction is given for qualities smaller than 30%.
The W-3 correlation predicts burnout onset always in the central channels and the DNBR values predicted go from 0,8 to 1,2 on the average.
All we have said before is clearly expressed in figures 3 to 6.

NON-UNIFORM TESTS

Channel B - Set I.
(tab. III, fig. 7)

This test-section is similar to the test section of set B tests, with obstructions in the flow area. These obstructions are obtained by the substitution of the ferrules by solid cylinders at each grid step in one of the central channels.
Experimental DNB appears to be influenced by this fact, and occurs in many tests on the rods surrounding the obstructed channel. MICRO-3 takes good account of the situation, and, by a comparison of the set I analysis results with similar tests of set B, we remark that there is a mass flow rate redistribution which puts the obstructed channel in a less favourable position with respect to the other central channels as far as enthalpy rise is concerned. As for DNB results, ΔH-FIAT correlation indicates DNB to occur in side channels, and the values go from 0,85 to 1,05.
W-3 correlation, for tests which fall in its quality validity range, indicates the obstructed subchannel as burnout channel (due to the mass flow rate which is little because of the mentioned redistribution). This is an indication of the fact that W-3 cold wall correction brings less penalty than ΔHFIAT. Values predicted of DNBR go from 0,8 to 1,0.

Channel B - Set II.1
(tab. IV, fig. 8 and 9)

In this set of experiments the central rod of set B is a cluster control rod (unheated) with a greater outer diameter. We have then a longitudinal flow area in the central channels smaller than in set B. This means a change in the mass flow rate distribution and the presence of cold wall correction in every subchannel. Experimentally DNB occurs always on the corner rod. MICRO-3 indicates transition of the maximum mass flow rate redistribution from the central channel, where it was localised in set B, to one of the side channels of set II.1. We have then a quite clear behavior of the correlations. ΔHFIAT (most of the runs are at high quality) DNBR results go from 0,8 to 1,0 for 84 ata, and from 0,8 to 1,1 for 132 ata, with one exception in which probably the combination of the parameters gives too much cold wall correction.
At a pressure of 132 ata the minimum DNBR predicted by ΔHFIAT correlation goes from corner to central subchannel as mass flow rate increases. This can be explained by the consideration that, at high mass flow rates, the effect caused by the redistribution becomes greater than the cold wall correction one. As for W-3 predictions, in the few tests which fall in its validity range, they are satisfactory giving DNBR values ranging from 1,0 to 1,2.

Channel B - Set II.2
(tab. V, fig. 10, 11)

The three unheated rods of this set have the effect to move DNB experimental signal toward the group of rods which are away from them; MICRO-3 agrees well with the experimental results.
As it can be seen from the example in Appendix B, the subchannel analysis acts in the way to have a mass flow rate redistribution with a peak in the central channels. Naturally, the most heated of these channels will have higher quality and probability of DNB. ΔHFIAT correlation gives DNBR values going from 0,85 to 1,15, with the minimum

DNBR location going from side to central channel as the mass flow rate increases.
W-3 indicates DNB to occur in the central channel in the 80% of the tests and the values go from 0,95 to 1,15.

Channel B - Set II.3 and II.4 (tab. VI-VII, fig. 12, 13, 14, 15)

This section has the four corner rods unheated, and three of the remaining rods with 23% power overload with respect to the two other ones.
The difference between the two sets is that the latter has a cluster control rod (unheated, with larger outer diameter) in a corner.
From the analysis point of view this represents a new fact: four subchannels with no heat addition, which are precisely the corner subchannels. The subchannel surrounded by the three averloaded rods, which are adjacent, is in the most unfavorable situation, and in effect DNB occurs experimentally always in the central overloaded rod.
MICRO-3 takes into account this situation and in each test we find (please note the two complete examples in Appendix B) a great difference in outlet quality from unheated to heated channels. The subchannel surrounded by the three overloaded rods has naturally the higher quality and also minimum DNBR value, both for ΔHFIAT and W-3 correlations.
The two examples in Appendix B relative to set II.3 and II.4 have approximatively the same input parameters. They help to understand the effect of the cluster control rod. The effect, of course, is localized in the adjacent subchannels for which we have a stronger redistribution of the mass flow rate in the set II.4. This acts in a way to adverse more and more the minimum DNBR channel of set II.4, since the outlet quality does not change much, but the mass flow rate becomes lower. Since great part of the tests are subcooled, this acts in a way to decrease the critical heat flux.
We must say that the growth of the outer diameter of the corner unheated rod, brings a stronger cold wall correction in the side subchannel interested

by it. For this fact in many of the set II.4 tests ΔHFIAT correlation (which has a greater sensibility to cold wall effect than W-3 corr.) gives the minimum of all DNBRs in the quoted sub channel.

If we stay strictly in the declared validity range of the correlations and cold wall corrections, ΔHFIAT results go from 1,1 to 1,25 and W-3 results go from 0,8 to 1,2.

Channel B - Set II.5 (tab. VIII and fig. 16 - 17)

In this set of tests the effect of a power radial step is taken into account. Experimental DNB occurs always on the most heated rod. MICRO-3 does not indicate great variations of the mass flow rate redistributions from the set B ones (i.e. from a radial uniform power distribution).
ΔHFIAT correlation gives minimum DNBR values in the DNB rod channels going from 0,9 to 1,3 (1,1 to 1,3 in the validity range of the cold wall correction). In effect, especially in the tests at 132 ata, the correlation, owing to the cold wall penalty, gives wall subchannel DNBRs slightly lower than the central channel ones.
It is not so for W-3 correlation, for which the minimum DNBR is always located in the central channel. Values go from 0,95 to 1,15, but there are only few points owing to the fact that there are few test in W-3 quality validity range.

Channel B - Set III (tab. IX and fig. 18 - 19 - 20)

This set is completely different from the others owing to the fact that axial heat flux is not uniform. The axial flux distribution is a chopped centered cosine with $\phi_{max}/\bar{\phi}$ (ratio of maximum value to average value) equal to 1,7 ; the exact axial shape is reported in figure 5 of Reference 7 . For the unheated rods, the rod configuration is similar to that relative to the set II.4. DNB occurs always in the central rod. In this case

MICRO-3 calculates DNBR values at each step using the local parameters given by previous thermohydrau lic calculations.
We shall have a different behaviour of our two main correlations, namely W-3 and ΔHFIAT. Since ΔHFIAT gives DNB in terms of a critical enthalpy rise, the minimum DNBR will be located at the end of the channels. On the other side W-3 predicts a critical heat flux; consequently the minimum DNBR will be located somewhere in the axial center of the sub channel (from our analysis the relative axial positions of minimum DNBR go from 0,57 to 0,68 on the average).
In table VIII and in the quoted figures we have reported DNBR values at the outlet for ΔHFIAT correlation, and the axial minimum for W-3, always in the subchannels in which experimental DNB has been detected.
Unfortunately, the tests at 84 ata, which are in ΔHFIAT quality validity range, are not in the cold wall correction's mass flow rate validity range.
The same consideration goes to the few tests at 132 ata which are not subcooled.
The DNBR values go from 1,2 to 1,4; however we must observe that even in these cases the DNBR in the wall subchannel of the cluster control rod (which has the greatest cold wall penalty) is smaller than in the central subchannel.
The same behavior was found in Set II.4.
W-3 has a wide number of tests falling in its quality validity range, but a part of them are out of range for mass flow rates. However, results are very good in general, going from 0,9 to 1,05 in the full validity range tests and from 0,95 to 1,3 in the partial validity range tests.
As for the prediction of the DNB axial location, diagram 20 shows the comparison of experimental and theoretical values.

GE correlation results

As said before, this correlation is appliable only to corner cells of our test section.

In its range of validity the DNBRs predicted go from 0,8 to 1,3 as we can see from diagram 21, relative to sets A and B.

CONCLUSION

In the present work the main purpose was to test the computer program MICRO-3, and, more in detail, the ΔHFIAT and W-3 correlations, for the prediction of the DNB conditions in a rod cluster.

We think this test has been successful for two reasons; first, the experimental program analyzed is various enough, and second, correlations and experimental tests have completely different origin.
The best final comment, to our opinion, are the two last Figures of the report.

Figure 22 illustrates DNB ratios for the tests in which the analysis has found DNB to occur in subchannels without cold walls; in it we can observe predictions from original correlations (no cold-wall penalty).

Figure 23 represents the summary of our entire analysis. The symbols used in these figures are the ones indicated in Fig. 1.

As we can very well see, the approximation is ±25% at a 98% confidence level.
Since in nuclear engineering the safety factor for DNBR is usually 30%, the approximation mentioned above is considered to be fully satisfactory.

REFERENCES

1. L.S. TONG - "DNB predictions for axially non uniform heat flux distribution" - WCAP 2815 Rev. 1 - September 1965.

2. G. PREVITI, R. RICCARDI, A. VALTANCOLI - "Critical heat fluxes prediction for forced convection boiling fluid flow" FIAT - Sezione Energia Nucleare, internal report.

3. JANNSSEN E. - ASME paper 63-WA-149.

4. JANNSSEN E. and KERVINEN J.A. - "Burnout conditions for non uniformely heated rod in annular geometry water at 1000 psia" - GEAP 3755 - June 1963.

5. TONG et al. - "Experimental determination of the departure from nucleate boiling in large rod bundles at high pressures" - 1967 WCAP 7045.

6. CAMPANILE et al. - "Forced convection Burnout and Hydrodynamic Instability Experiments for Water at High Pressure; Part VI: Burnout Heat Flux Measurements on 9 Rod-Bundles with Longitudinally and Transversally Uniform Heat Generation" - EUR 4468e.

7. CAMPANILE et al. - "Forced convection Burnout and Hydrodynamic Instability Experiments for Water at High Pressure; Part VII: Burnout Heat Flux Measurements on 3 x 3 rod bundles with non-uniform heat generation" - EUR 4514e.

APPENDIX A

MICRO-3 PROGRAM DESCRIPTION

MICRO-3 is a computer program which performs a detailed thermo-hydraulic subchannel analysis.
The computed local density, mass velocity, enthalpy, steam quality are used for the calculation of DNBRs.

As we know, in the subchannel analysis, a portion of fuel assembly, a fuel assembly, or a group of fuel assemblies, is considered as a channel. In our case, within a channel the flow properties at each elevation are considered to be uniform. Furthermore, at each elevation, pressure is considered to be the same in all the subchannels, because within an assembly the lateral resistance of the fuel rod lattice between subchannels is very small and thus only a small pressure gradient can exist across the assembly. MICRO-3 obtains the overall mass balance by means of a control volume approach: the assembly is divided into a series of axially segmented channels with fixed boundaries. The computations determine successively the change in conditions between the inlet and outlet of each axial segmented channel and allow for cross flow among channels. For these reasons, use of radial simmetry simplifies the analysis.

For the use of this code, the necessary operations are:

- division of the region into a certain number of adjacent channels;
- division of each channel into a certain number of axial increments of equal length.

Within each channel the parameters associated with the fluid are considered to vary in the vertical direction only. Adjacent channels exchange mass, energy and momentum.

The exchange processes are governed by the laws of conservation of mass, energy and momentum.

Let us examine now the fundaments of this analysis; the symbols are those indicated in the sketch of next page.

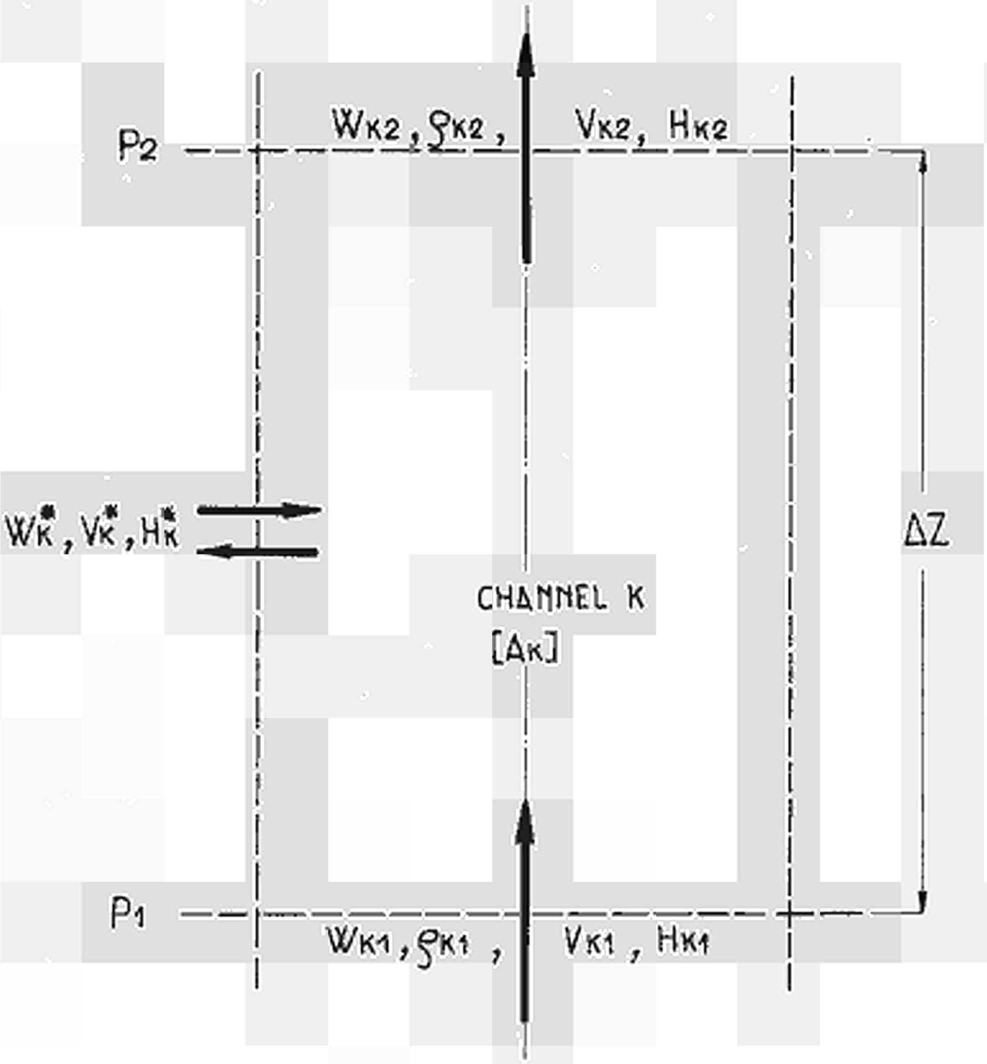

MICRO-3 Program Schematization at a given elevation in a given subchannel.

Since the array arrangement in the code is rectangular, a given channel may be coupled to as many as four other channels.

- Mass balance. In channel K at elevation "1" we have, for a mass balance:

$$W_{k1} + W_k^* = W_{k2} ;$$
$$A_k V_{k1} \rho_{k1} + W_k^* = A_k V_{k2} \rho_{k2} ; \qquad (1)$$

were V is the local velocity, ρ is the local density, W is the mass flow rate, and A is the subchannel area.

- A heat balance gives:

$$A_k V_{k1} \rho_{k1} H_{k1} + Q_k + (TC)_k + W_k^* H_k^* = A_k V_{k2} \rho_{k2} H_{k2} ; \qquad (2)$$

H_{k1} and H_{k2} are the step inlet and outlet coolant enthalpies respectively.

Q_k is the heat flux in channel K.

$(TC)_k$ is the heat exchange rate due to thermal diffusion between channels J and K.

H_k^* is the enthalpy associated with the cross flow.

TC, thermal diffusion coefficient, is determined from:

$$(TC)_k = \sum_i w'_k \cdot \Delta z \cdot (H_i - H_k) ;$$

w' is the flow exchange rate per unit length.

Δz is the height of the axial length step.

H_i and H_k are defined as the mean enthalpies in channels I and K. The index i refers to each channel surrounding channel K.

Values of w' are determined experimentally (reports WCAP-708/ NACA-TN 3663/WCAP 1783) in terms of a mixing coefficient $\varepsilon = w'/\rho$ and of the fact that the Peclet modulus ε/Vl is relatively independent of coolant parameters for a given geometry. For our particular geometry (3 x 3 rod bundle) experiments have suggested the use of a value of 0.014296 for the above mentioned modulus or "thermal diffusion coefficient".

- Then a <u>momentum balance</u> for the element at height "1" in channel K gives:

$$A_K P_1 + A_K \rho_{K1} \frac{V_{K1}^2}{g_c} + W_K^* \frac{V_K^*}{g_c} = A_K P_2 + A_K \rho_{K2} \frac{V_{K2}^2}{g_c} + K_K A_K \bar{\rho}_K \frac{\bar{V}_K^2}{2 g_c} + A_K \bar{\rho}_K \Delta z \frac{g}{g_c} \quad (3)$$

where $\bar{\rho}_K$ and $\bar{V}_K$ are defined as mean values in the sub-channel at the given elevation.

- <u>Cross-flow rate</u>

The values of V_k^* and H_k^* are weighted average values determined from the enthalpies and mass flow rates at the inlet and outlet of channel k and its adjacent channels. The equation for H_k^* is :

$$H_K^* = \frac{1}{2} \Sigma_i \left[|X_{iK}| \left(\bar{H}_i + \bar{H}_K \right) + X_{iK} \left(\bar{H}_i - \bar{H}_K \right) \right] \Big/ \Sigma_i |X_{iK}| \quad (4)$$

where the index i refers to each channel surrounding channel k, and the weighting factor X_{ik} represents the net gain in the rate of mass flow per unit cell between channels i and k. A similar equation for V_k^* may be written in terms of V_i and V_k.

- <u>Models</u> used in the programs:

a) Local Boiling and Bulk Boiling Voids.

The correlations of Bowring are used, with the consideration of three distinct regions, which are:

- Highly subcooled local boiling region.
- Slightly subcooled local boiling region.
- Bulk-boiling region.

b) Two-phase pressure drop calculation.

For single-phase flow Moody friction factors are used.

For two-phase Owens' method, which assumes a homogeneous flow model in which the two-phase friction factor is equal to the single-phase friction factor, is preferred to Martinelli-Nelson's.

The calculation procedure is as follows.
Combination of equations (1) and (2) eliminates W_k^* and gives an equation in terms of increments of density and velocity.
Similarly equation (3) may be written in form of increments of density, velocity and pressure.
Since the sum of the cross flows for all the subchannels must be zero, equation (1) may be used to obtain an additional equation.
We have at last a system of $2n+1$ equations for each length step, where n is the number of the subchannels. This system is non-linear; so an iteration procedure is used to solve it. The convergence check is determined by the additional equation upmentioned.
The resulting density, velocity, and static pressure at the top of the length step are used as inputs for the next length step.
This procedure is continued stepwise up to the top of the core.

For grid-steps, the program acts a dilution of the localized pressure loss among the steps before and behind, and the grid-step itself. This procedure is actuated for a better physical representation of the mass velocity changes in the grid zones.

A P P E N D I X B

MICRO-3 CODE SUBCHANNEL DIVISION AND MAIN OUTPUT EXAMPLES

Channel A Set. 0 Test 57 (20-6-68)

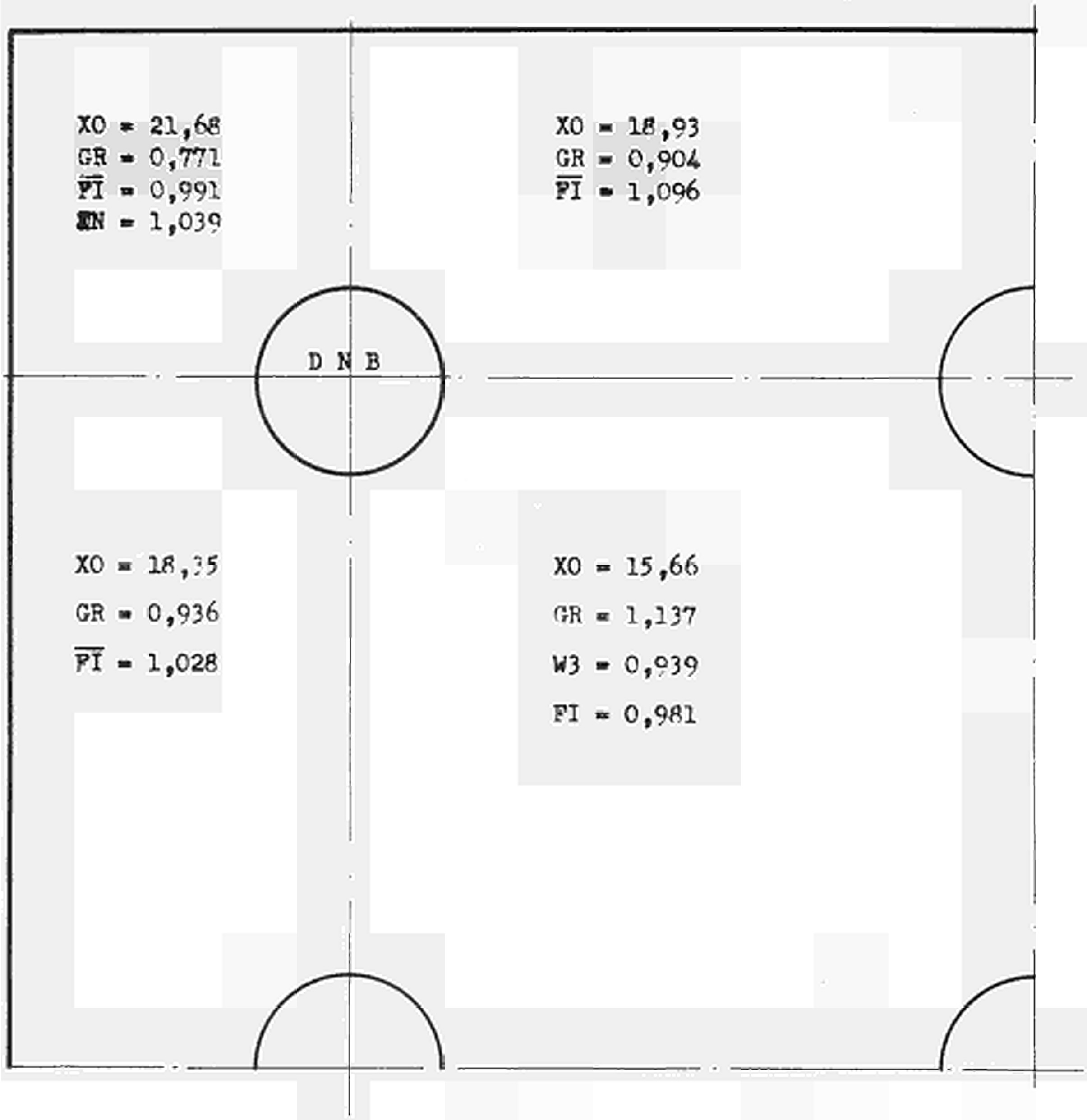

Pressure : 115 ata
Mass flow rate 157 gr/cm^2 s
Inlet temperature 282,7 °C

XO = Outlet quality (%)
GR = Outlet/inlet mass flow rate
W3 = W-3 corr. DNB ratio

FI = FIAT corr. DNB ratio
JN = JANNSEN corr. DNB ratio
‾ = DNB ratio with cold wall correction

Channel B Set 0.   TEST 115 (6-2-68)

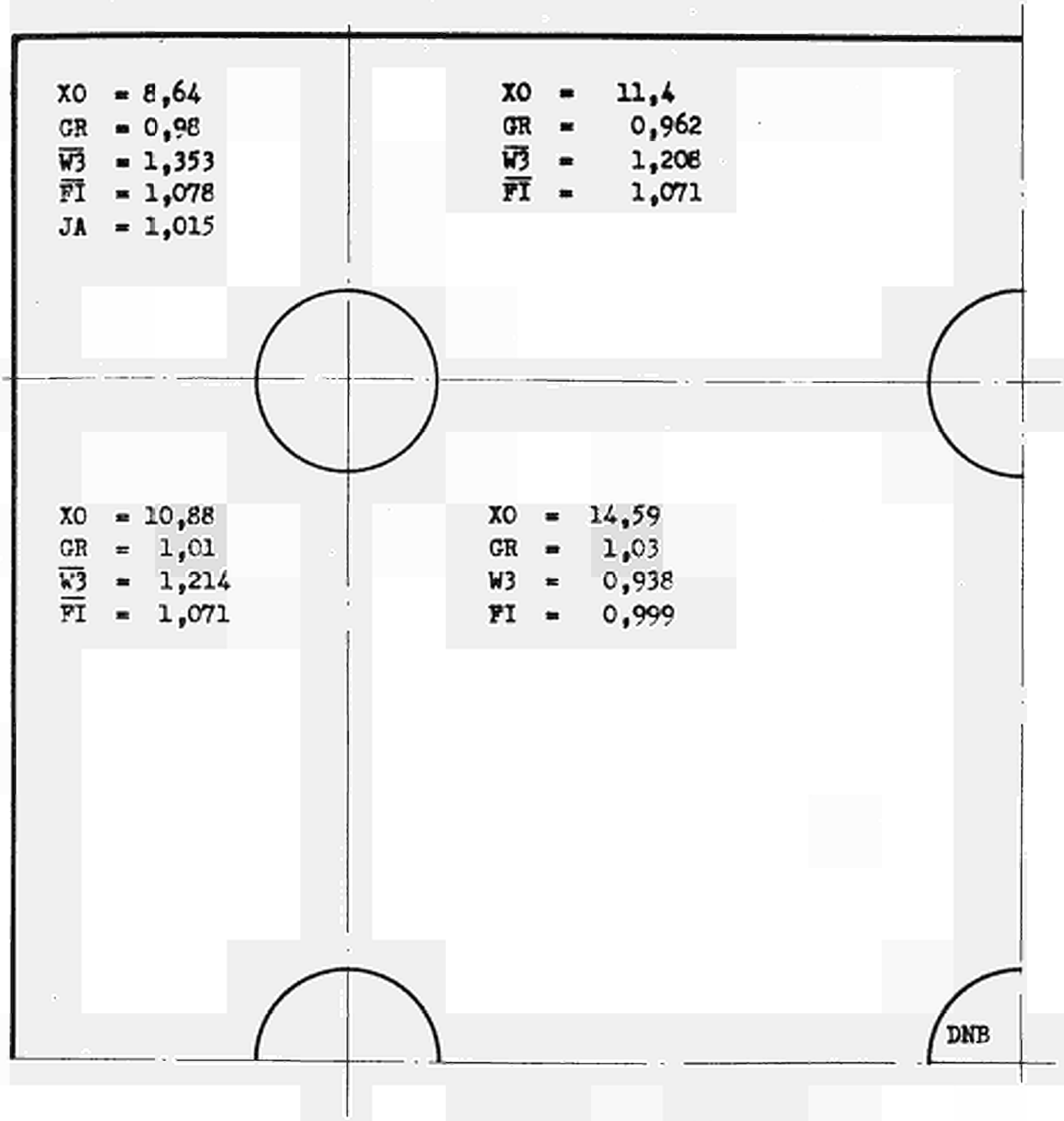

Pressure : 132 ata
Mass flow rate : 157 gr/cm^2 s
Inlet temperature : 308,4 °C

XO = Outlet quality (%)
GR = Outlet/inlet mass flow rate
W3 = W-3 corr. DNB ratio
FI = FIAT corr. DNB ratio
JA = JANNSEN corr. DNB ratio
$\overline{}$ = DNB ratio with cold wall correction

Channel B Set I. Test 90 (9-8-68)

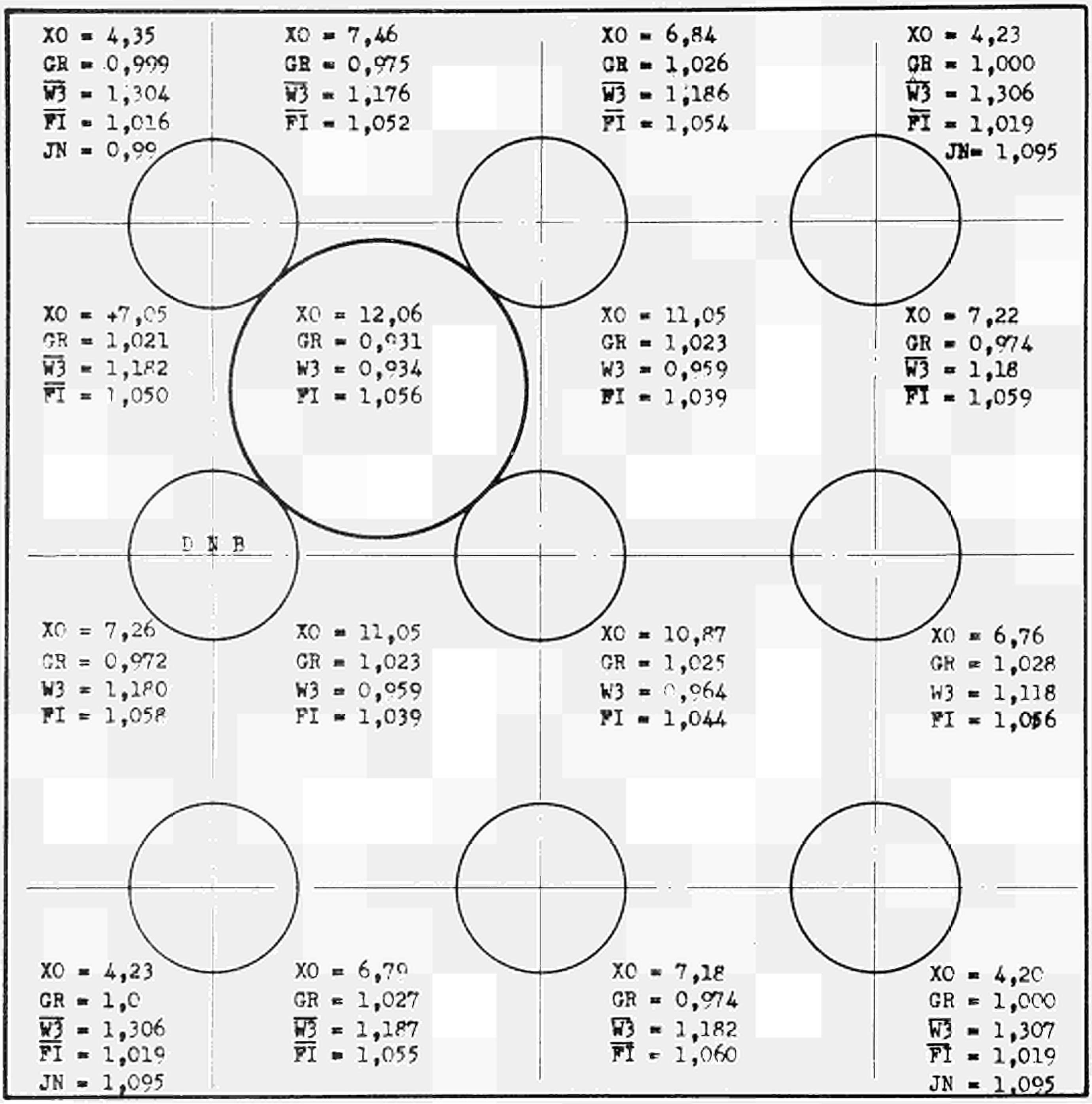

Pressure 132 ata
Mass flow rate 161,3 gr/cm^{2}s
Inlet temperature 290°C

XO = Outlet quality (%)
GR = Outlet/inlet mass flow rate
W3 = W-3 corr. DNB ratio
FI = Fiat corr. DNB ratio
JN = JANNSEN corr. DNB ratio
‾ = DNB ratio with cold wall correction

Channel B Set. II-1   Test 54 (23-9-68)

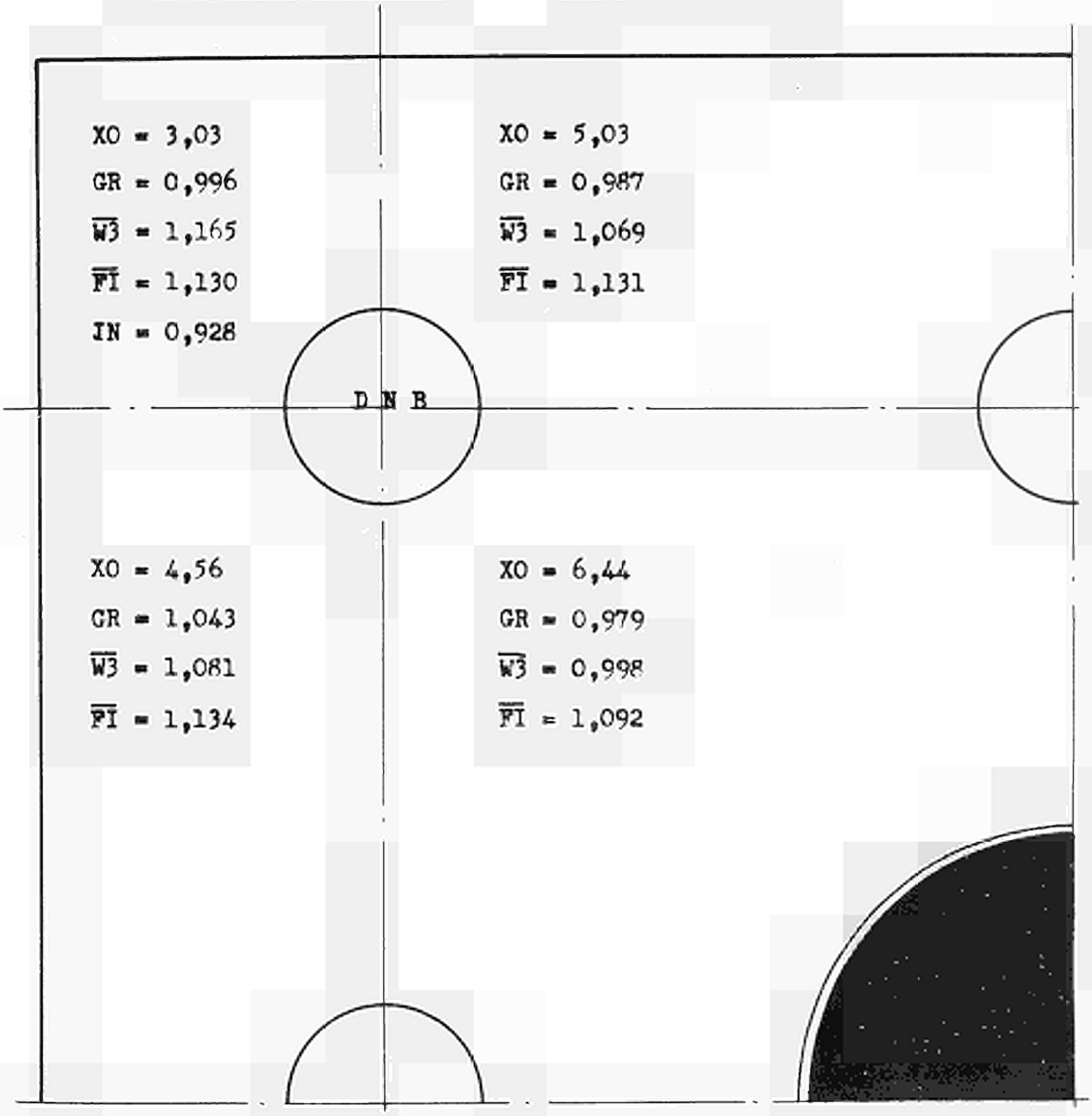

Pressure 132 ata
Mass flow rate 230,9 gr/cm^{2}s
Inlet temperature 300,2 °C

XO = Outlet quality (%)
GR = Outlet/inlet mass flow rate
W3 = W-3 corr. DNB ratio

FI = Fiat corr. DNB ratio
JN = JANNSEN corr. DNB ratio
— = DNB ratio with cold wall correction

Channel B Set II.2 **Test 64 (23-10-68)**

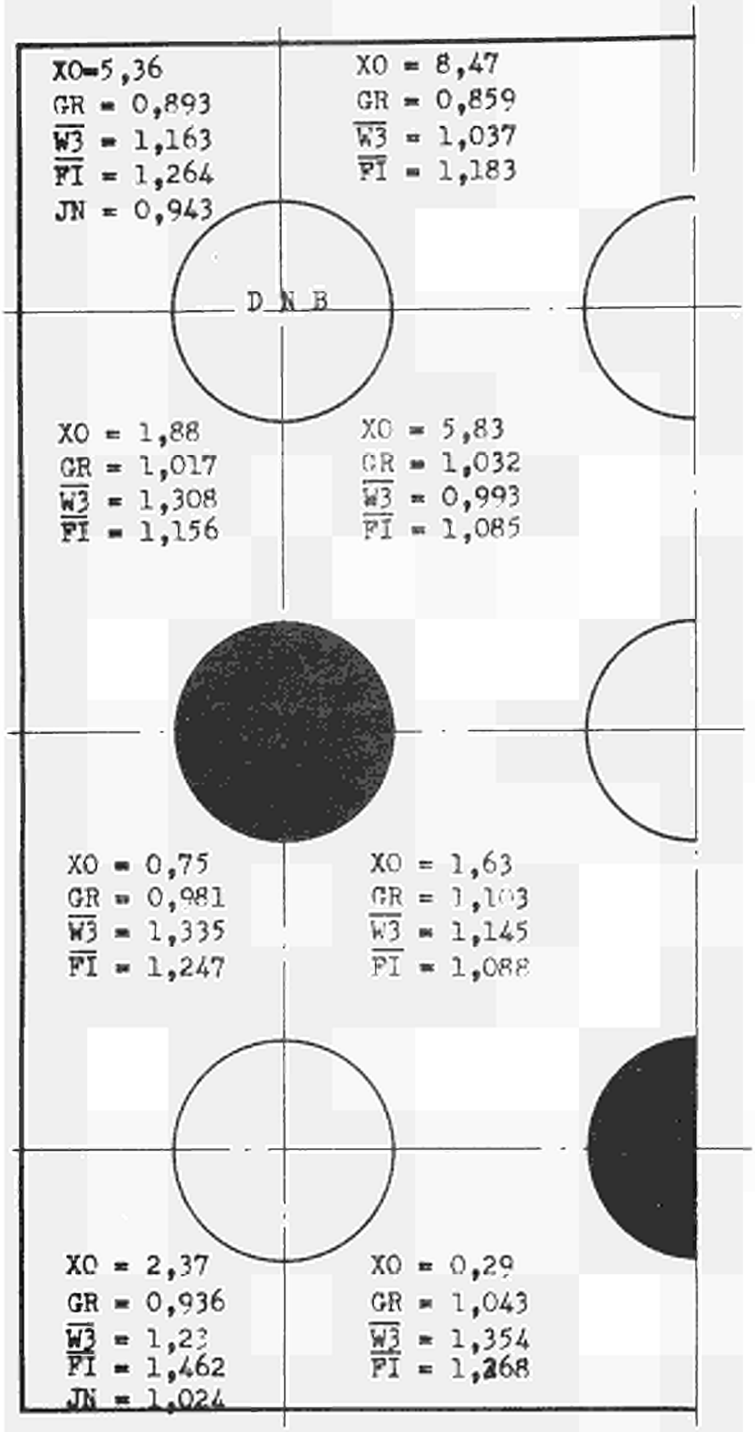

Pressure	132 ata
Mass flow rate	233 gr/cm^{2}s
Inlet temperature	311,2°C

XO = Outlet quality (%)
GR = Outlet/inlet mass flow rate
W3 = W-3 corr. DNB ratio
FI = Fiat corr. DNB ratio
JN = JANNSEN corr.DNB ratio
=DNB ratio with cold wall correction

Channel B Set. II-3 **Test 10 (2-4-69)**

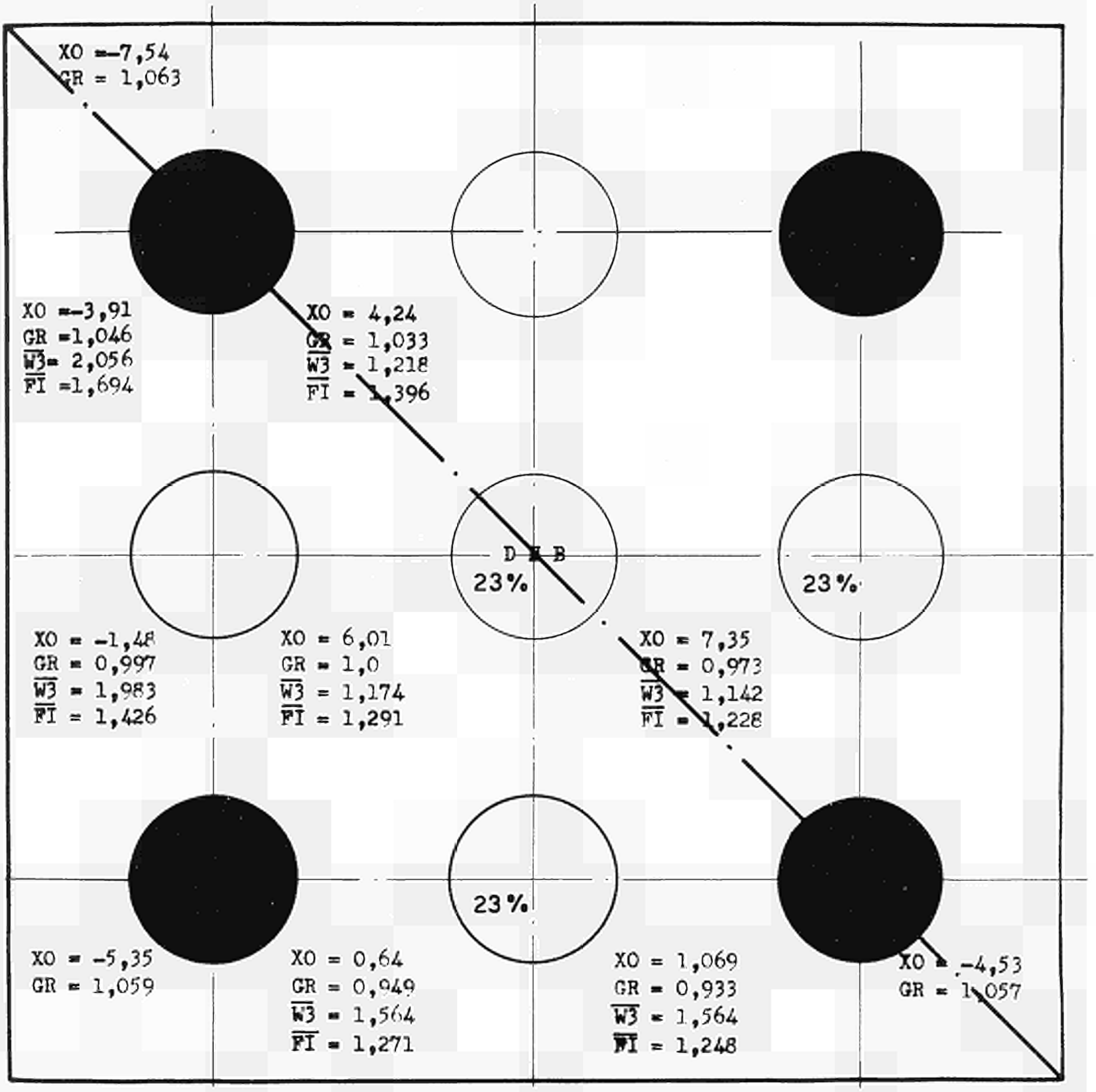

Pressure 132 ata
Mass flow rate 157 gr/cm^{2}s
Inlet temperature 308,5 °C

XO = Outlet quality (%)
GR = Outlet/inlet mass flow rate
W3 = W-3 corr. DNB ratio

FI = Flat corr. DNB ratio
JA = JANNSEN corr. DNB ratio
$\overline{}$ = DNB ratio with cold wall correction

Channel B Set. II-4 Test 87 (25-11-68)

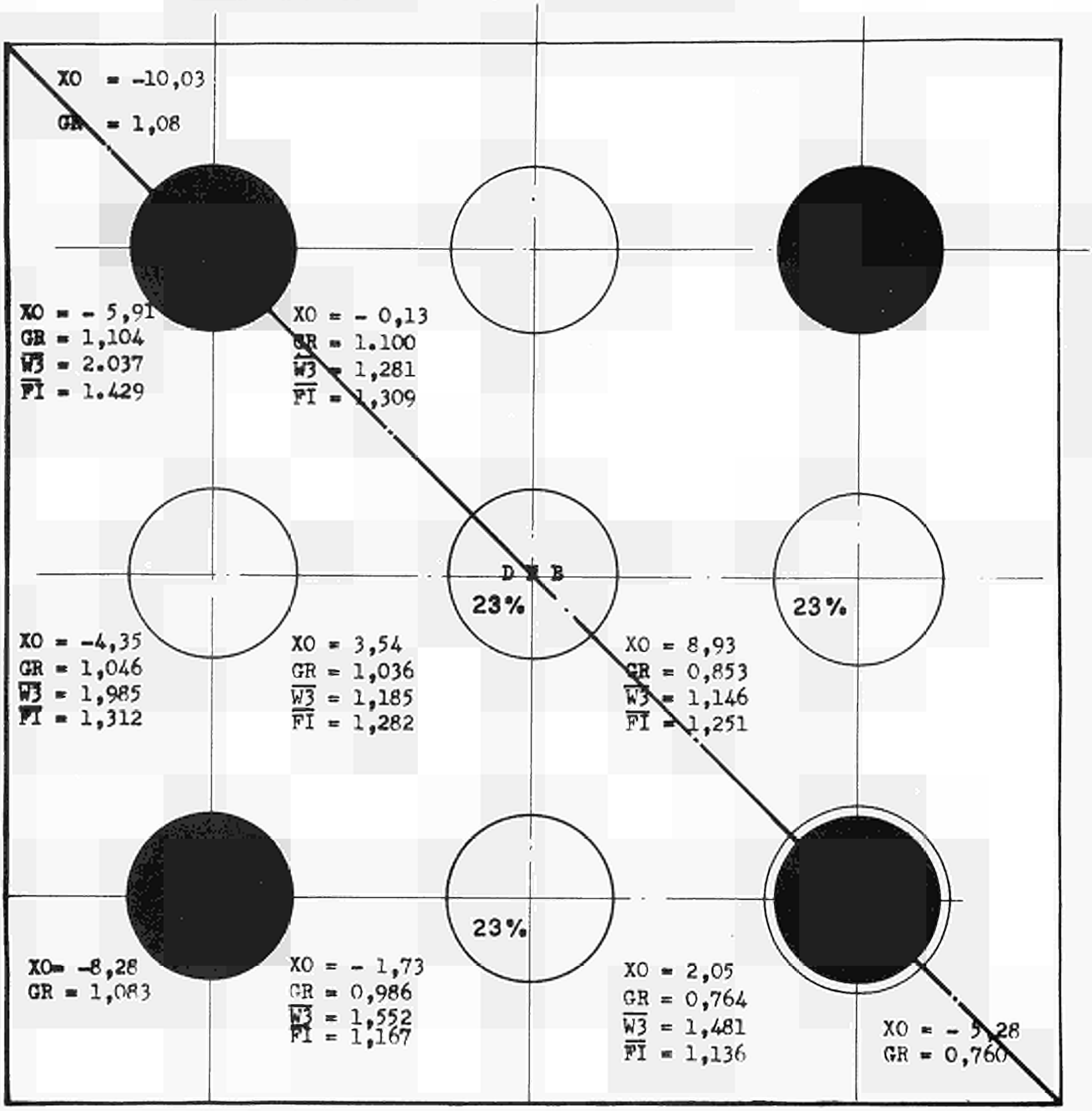

Pressure : 132 ata
Mass flow rate : 157,2 gr/cm^{2}s
Inlet temperature : 301,5 °C

XO = Outlet quality (%)
GR = Outlet/inlet mass flow rate
WB = W-3 corr. DNB ratio

FI = Fiat corr. DNB ratio
JA = JANNSEN corr. DNB ratio
— = DNB ratio with cold wall correction

Channel B Set II.5 **Test 39 (16-12-68)**

Pressure	84 ata
Mass flow rate	161,6 $gr/cm^2 s$
Inlet temperature	319,0 °C

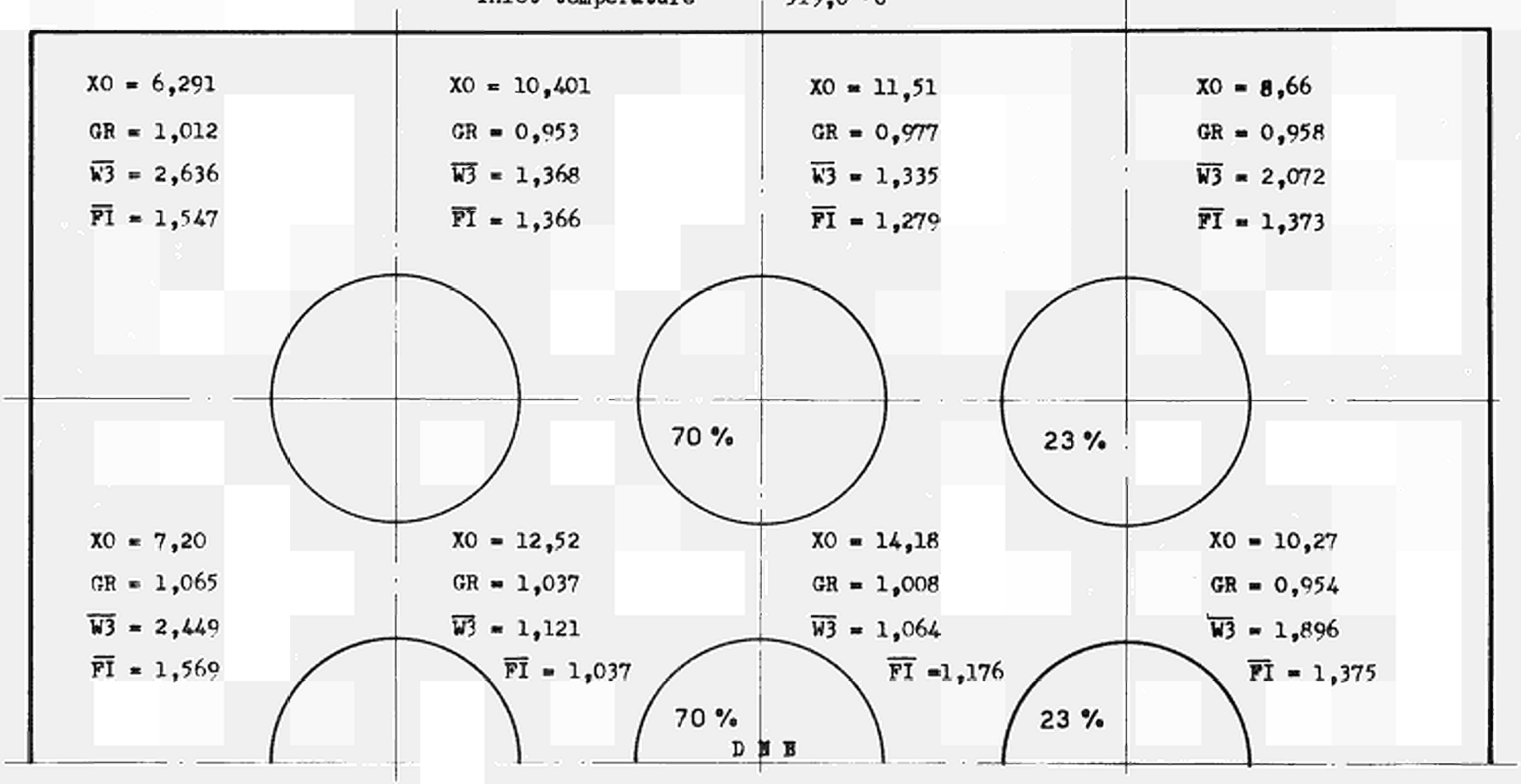

XO = Outlet quality (%)
GR = Outlet/inlet mass flow rate

W3 = W-3 corr. DNB ratio
FI = FIAT corr. DNB ratio

JA = JANSSEN corr. DNB ratio
$\overline{\quad}$ = DNB ratio with cold wall correction

Channel B Set III. Test 11 (11-11-69)

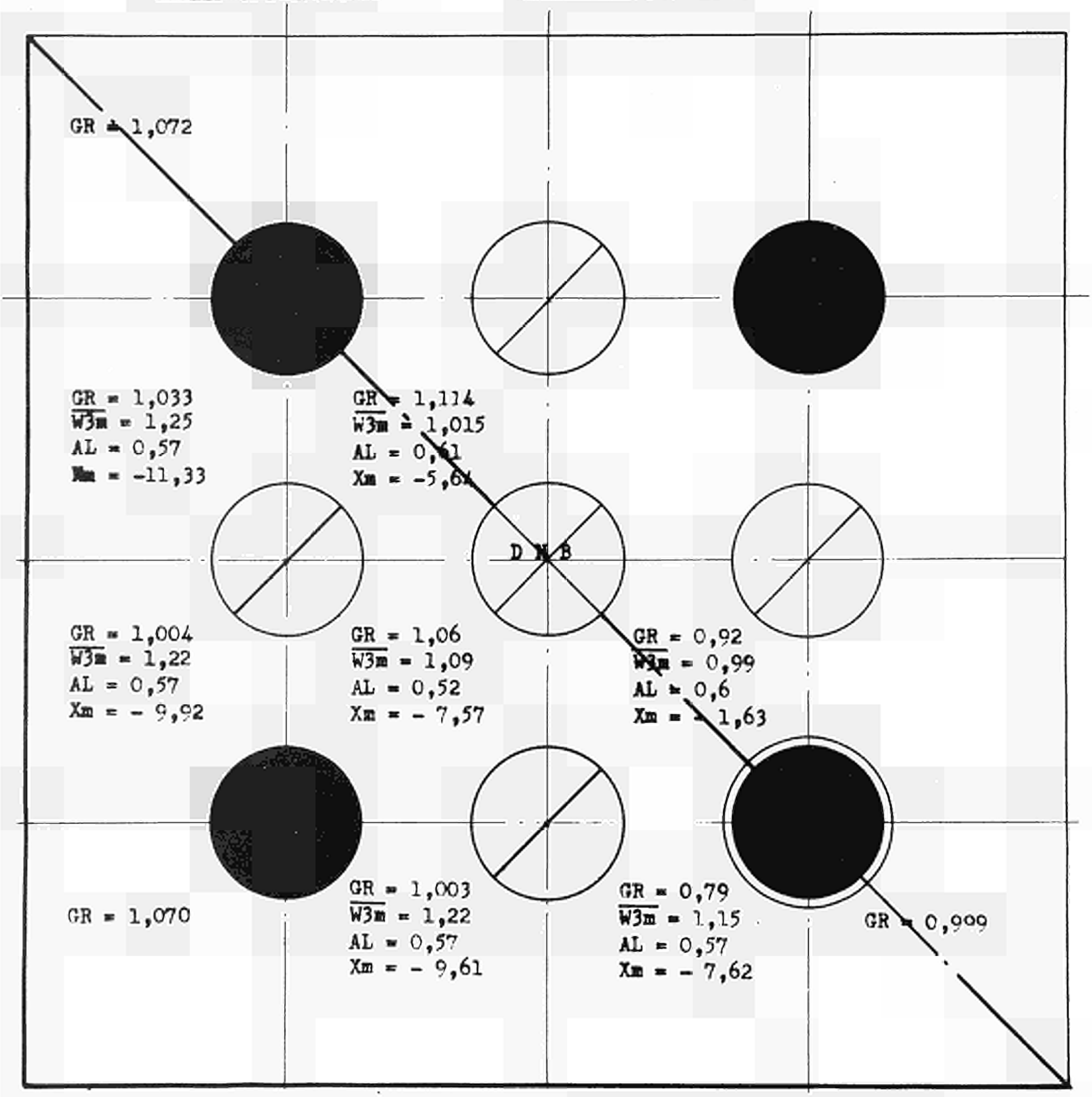

Pressure	132 ata
Mass flow rate	156,9 gr/cm^{2}s
Inlet temperature	301,2 °C

GR = Outlet/inlet mass flow rate
W3m = minimum axial DNB ratio according to W-3 correl.
AL = axial position (%) of minimum DNBR
Xm = Local quality at AL
$\overline{\text{W3m}}$ = W3 DNBR with cold wall correction

TABLES

TABLE I - EXPERIMENTAL DATA AND ANALYTICAL RESULTS FOR CHANNEL A SET. 0

EXPERIMENTAL DATA							ANALYTICAL RESULTS							
Run	Nominal pressure ata	Mass flow rate g/cm²s	Inlet temperature °C	Critical heat flux W/cm²	Average exit quality %	B.O. Rods position in the lattice	ΔH-FIAT DNBR	Subchannel local quality %	G out / G in	Subchannel critical heat flux location	W-3 DNBR	Subchannel local quality %	G out / G in	Subchannel critical heat flux location
74 (25-6-68)	84	52,11	261,2	121,5	49,95	1	0,882 ++	59,66	0,74	CORNER CELL	-	-	-	-
27 (25-6-68)	"	50,91	233,5	121,8	42,08	1	0,911 ++	53,83	0,73	"	-	-	-	-
15 (25-6-68)	"	52,03	209,0	141,3	42,86	1	0,859 ++	55,89	0,74	"	-	-	-	-
169 (25-6-68)	"	93,65	284,0	148,3	37,59	1	0,922 ++	43,05	0,76	"	-	-	-	-
109 (25-6-68)	"	91,79	280,2	159,6	40,04	1	0,876 ++	46,23	0,77	"	-	-	-	-
46 (25-6-68)	"	92,49	266,5	161,6	35,79	1	0,913 ++	41,54	0,77	"	-	-	-	-
190 (25-6-68)	"	157,59	291,2	168,5	26,29	1	1,008	29,63	0,78	"	-	-	-	-
137 (25-6-68)	"	154,79	285,2	174,4	25,59	1	1,003	28,94	0,78	"	-	-	-	-
68 (20-6-68)	115	51,07	294,9	100,7	49,45	1	0,816 ++	60,76	0,72	"	-	-	-	-
34 (19-6-68)	"	51,96	252,5	119,8	42,56	1	0,797 ++	57,87	0,72	"	-	-	-	-
9 (19-6-68)	"	51,49	231,5	128,9	41,03	1	0,798 ++	55,89	0,71	"	-	-	-	-
87 (20-6-68)	"	96,40	293,7	130,0	29,85	1	0,927 ++	35,44	0,75	"	-	-	-	-
16 (20-6-68)	"	93,08	265,7	151,6	26,87	1	0,895 ++	34,11	0,75	"	-	-	-	-
27 (19-6-68)	"	92,93	243,7	184,1	23,3	1	0,828 ++	38,08	0,75	"	-	-	-	-
76 (20-6-68)	"	158,86	293,7	154,6	18,43	1	1,001	16,52	1,14	CENTRAL CELL	0,998	16,52	1,14	CENTRAL CELL

\+ Out of range for mass flow rate

++ Out of range for mass flow rate in cold wall correction

EXPERIMENTAL DATA							ANALYTICAL RESULTS							
Run	Nominal pressure ata	Mass flow rate g/cm^2s	Inlet temperature °C	Critical heat flux W/cm^2	Average exit quality %	B.O. Rods position in the lattice	ΔH-FIAT DNBR	Subchannel local quality %	$\frac{G\ out}{G\ in}$	Subchannel critical heat flux location	W - 3 DNBR	Subchannel local quality %	$\frac{G\ out}{G\ in}$	Subchannel critical heat flux location
57 (20-6-68)	115	156,96	282,7	173,6	17,72	1	0,981	15,66	1,14	CENTRAL CELL	0,939	15,66	1,14	CENTRAL CELL
29 (20-5-68)	"	153,63	272,0	180,0	13,45	1	1,015	13,17	1,14	"	0,992	13,17	1,14	"
58 (7-6-68)	132	50,38	288,2	98,0	43,63	1	0,796 ++	57,92	0,68	CORNER CELL	-	-	-	-
45 (7-6-68)	"	50,51	270,5	106,3	41,48	1	0,786 ++	56,97	0,67	"	-	-	-	-
9 (7-6-68)	"	52,46	240,0	118,5	33,61	1	0,799 ++	50,73	0,64	"	-	-	-	-
112 (7-6-68)	"	89,25	304,5	114,2	28,0	1	0,910 ++	35,84	0,73	"	-	-	-	-
19 (6-6-68)	"	90,79	279,8	130,2	22,5	1	0,917 ++	30,52	0,72	"	-	-	-	-
33 (6-6-68)	"	94,81	251,0	165,0	13,78	1	0,863 ++	30,09	0,72	"	-	-	-	-
95 (7-6-68)	"	161,09	305,0	145,1	15,28	1	0,948	14,51	1,14	CENTRAL CELL	0,957	14,51	1,14	CENTRAL CELL
41 (7-6-68)	"	154,31	268,0	177,6	7,49	1	1,031	5,89	1,17	"	1,107	5,89	1,17	"
125 (7-6-68)	"	226,46	309,5	163,1	10,65	1	0,915	11,63	1,14	"	0,911	11,63	1,14	"
87 (7-6-68)	"	226,38	293,7	183,3	6,64	1	0,999	6,55	1,15	"	1,027	6,55	1,15	"
60 (18-6-68)	144	50,82	307,7	87,3	44,61	1	0,787 ++	58,26	0,66	CORNER CELL	-	-	-	-
49 (14-6-68)	"	51,78	285,2	97,2	38,88	1	0,791 ++	54,69	0,63	"	-	-	-	-
30 (12-6-68)	"	50,55	256,0	108,5	35,06	1	0,778 ++	53,36	0,60	"	-	-	-	-

\+ Out of range for mass flow rate

++ Out of range for mass flow rate in cold wall correction

TABLE I - (FOLLOWS)

EXPERIMENTAL DATA							ANALYTICAL RESULTS							
Run	Nominal pressure ata	Mass flow rate $g/cm^2 s$	Inlet temperature °C	Critical heat flux W/cm^2	Average exit quality %	B.O. Rods position in the lattice	ΔH-FIAT DNBR	Subchannel local quality %	$\frac{G_{out}}{G_{in}}$	Subchannel critical heat flux location	W-3 DNBR	Subchannel local quality %	$\frac{G_{out}}{G_{in}}$	Subchannel critical heat flux location
67 (14-6-68)	144	94,24	309,8	110,2	25,15	1	0,920 ++	32,41	0,72	CORNER CELL	-	-	-	-
25 (14-6-68)	"	94,46	290,5	124,1	21,18	1	0,919 ++	28,46	0,71	"	-	-	-	-
15 (12-6-68)	"	93,59	251,2	146,2	11,72	1	0,905 ++	20,69	0,67	"	1,172 +	8,4	1,19	CENTRAL CELL
81 (14-6-68)	"	154,25	317,7	127,9	16,8	1	0,878	16,29	1,15	CENTRAL CELL	0,865	16,29	1,15	"
95 (14-6-68)	"	224,28	315,3	152,7	10,72	1	0,929	9,68	1,14	"	0,954	9,68	1,14	"
36 (14-6-68)	"	223,82	294,9	176,6	3,64	1	1,054	2,69	1,15	"	1,134	2,69	1,15	"

\+ Out of range for mass flow rate

++ Out of range for mass flow rate in cold wall correction

TABLE II - EXPERIMENTAL DATA AND ANALYTICAL RESULTS FOR CHANNEL B SET. U

EXPERIMENTAL DATA							ANALYTICAL RESULTS							
Run	Nominal pressure ata	Mass flow rate g/cm^2s	Inlet temperature °C	Critical heat flux W/cm^2	Average exit quality %	B.O. Rods position in the lattice	ΔH-FIAT DNBR	Subchannel local quality %	$\frac{G_{out}}{G_{in}}$	Subchannel critical heat flux location	W-3 DNBR	Subchannel local quality %	$\frac{G_{out}}{G_{in}}$	Subchannel critical heat flux location
27 (15-7-69)	84	48,3	283,7	120,3	50,5	1	0,967 ++	41,83	0,93	CORNER CELL	-	-	-	-
97 (7-2-68)	"	50,0	269,5	133,9	50,3	1-2	0,911 ++	42,81	0,93	"	-	-	-	-
9 (4-3-68)	"	49,8	242,6	151,0	48,9	1-2-9	0,878 ++	39,42	0,93	"	-	-	-	-
54 (4-3-68)	"	51,1	217,9	165,0	45,3	1-2-9	0,853 ++	35,77	0,92	"	-	-	-	-
48 (22-5-69)	"	93,1	283,8	168,3	35,0	1	0,932 ++	29,28	0,98	"	-	-	-	-
54 (22-5-69)	"	90,2	270,0	181,2	34,8	1	0,909 ++	27,52	0,99	"	-	-	-	-
23 (23-5-69)	"	92,4	242,0	203,1	28,9	2-9	0,979 ++	26,83	1,02	SIDE CELL	-	-	-	-
35 (17-7-69)	"	90,3	220,5	211,6	25,6	9	1,153	30,71	0,99	CENTRAL CELL	-	-	-	-
49 (29-7-69)	"	157,0	283,0	207,2	23,6	9	0,998	27,45	1,00	"	-	-	-	-
37 (29-7-69)	"	155,9	269,6	220,7	21,3	9	1,051	24,69	0,99	"	-	-	-	-
19 (29-7-69)	"	156,3	242,5	245,0	15,1	9	1,099	19,07	0,97	"	-	-	-	-
56 (29-7-69)	"	156,9	219,2	269,9	11,2	9	1,121	15,47	0,90	"	0,902	15,47	0,90	CENTRAL CELL
18 (30-7-69)	"	223,4	284,5	220,0	17,0	9	1,020	19,12	1,01	"	-	-	-	-
4 (30-7-69)	"	222,0	270,0	240,6	14,6	9	1,050	16,24	0,99	"	0,861	16,24	0,99	CENTRAL CELL
31 (15-2-68)	100	49,5	274,9	131,9	50,4	1-9	0,844 ++	43,17	0,90	CORNER CELL	-	-	-	-

\+ Out of range for mass flow rate

++ Out of range for mass flow rate in cold wall correction

TABLE II - (FOLLOWS)

EXPERIMENTAL DATA							ANALYTICAL RESULTS							
Run	Nominal pressure ata	Mass flow rate $g/cm^2 s$	Inlet temperature °C	Critical heat flux W/cm^2	Average exit quality %	B.O. Rods position in the lattice	ΔH-FIAT DNBR	Subchannel local quality %	$\frac{G\ out}{G\ in}$	Subchannel critical heat flux location	W - 3 DNBR	Subchannel local quality %	$\frac{G\ out}{G\ in}$	Subchannel critical heat flux location
43 (1[illegible]-2-68)	100	48,9	259,8	139,0	49,5	1-9	0,[illegible]44 ++	38,71	0,89	CORNER CELL	-	-	-	-
38 (5-3-68)	"	49,2	258,9	139,4	48,4	1-2-9	0,845 ++	38,42	0,89	"	-	-	-	-
64 (5-3-68)	"	49,6	258,4	138,4	47,4	1-2-9	0,849 ++	37,88	0,89	"	-	-	-	-
49 (5-3-68)	"	49,8	252,5	140,6	45,6	9	1,080	50,82	1,08	CENTRAL CELL	-	-	-	-
95 (15-2-68)	"	93,2	296,7	148,5	32,2	1-2	0,922 ++	27,51	0,97	CORNER CELL	-	-	-	-
65 (15-2-68)	"	92,2	282,5	159,1	29,8	9	1,033	34,11	1,03	CENTRAL CELL	-	-	-	-
20 (15-2-68)	"	94,3	265,4	171,7	25,1	9	1,047	31,38	1,02	"	-	-	-	-
62 (14-2-68)	115	50,2	301,5	111,2	48,7	1-2-9	0,852 ++	41,80	0,88	CORNER CELL	-	-	-	-
14 (5-3-68)	"	51,0	273,5	127,3	44,6	9	0,971	50,61	1,09	CENTRAL CELL	-	-	-	-
9 (14-2-68)	"	51,3	241,5	139,4	37,4	9	1,000	44,09	1,10	"	-	-	-	-
85 (14-2-68)	"	92,7	301,2	136,5	28,6	9	0,976	32,01	1,04	"	-	-	-	-
51 (14-2-68)	"	93,9	276,8	157,8	24,3	9	0,996	27,93	1,03	"	-	-	-	-
15 (20-5-69)	132	49,7	301,5	100,1	39,9	9	0,945	44,26	1,12	"	-	-	-	-
26 (20-5-69)	"	50,0	260,7	119,8	32,7	9	0,957	37,25	1,12	"	-	-	-	-
94 (19-1-69)	"	50,0	253,0	126,5	33,8	9	0,934	36,41	1,11	"	-	-	-	-

+ Out of range for mass flow rate

++ Out of range for mass flow rate in cold wall correction

TABLE II - (FOLLOWS)

EXPERIMENTAL DATA							ANALYTICAL RESULTS							
Run	Nominal pressure ata	Mass flow rate $g/cm^2 s$	Inlet temperature °C	Critical heat flux W/cm^2	Average exit quality %	B.O. Rods position in the lattice	ΔH-FIAT DNBR	Subchannel local quality %	$\frac{G\ out}{G\ in}$	Subchannel critical heat flux location	W-3 DNBR	Subchannel local quality %	$\frac{G\ out}{G\ in}$	Subchannel critical heat flux location
25 (13-5-69)	132	49,5	221,0	139,8	28,6	9	0,953	33,10	1,10	CENTRAL CELL	-	-	-	-
94 (6-?-68)	"	93,6	305,0	118,2	23,4	9	0,954	26,25	1,05	"	-	-	-	-
25 (22-1-68)	"	92,4	265,7	146,5	12,0	9	1,047	15,47	1,03	"	0,994 +	15,74	1,03	CENTRAL CELL
50 (21-5-68)	"	92,1	259,6	149,6	10,4	9	1,061	14,20	1,02	"	1,034 +	14,20	1,02	"
28 (22-5-69)	"	91,8	204,0	185,7	- 0,8	9	1,097	3,02	1,02	"	1,172 +	3,02	1,02	"
17 (29-5-69)	"	131,8	301,5	144,4	14,0	9	0,984	16,78	1,02	"	0,872	16,78	1,02	"
27 (29-5-69)	"	133,1	271,0	170,0	5,8	9	1,062	8,54	1,03	"	1,028	8,54	1,03	"
8 (30-5-69)	"	132,7	233,7	197,8	- 3,5	9	-	-	-	-	1,186	- 1,108	1,01	"
115 (6-2-68)	"	156,9	308,4	142,6	12,9	9	0,999	14,58	1,03	CENTRAL CELL	0,937	14,58	1,03	"
18 (12-6-69)	"	153,7	260,5	197,5	1,4	9	1,094	2,7	1,03	"	1,062	2,7	1,03	"
47 (12-6-69)	"	148,4	219,2	235,3	- 7,0	9	-	-	-	-	1,193	- 6,99	1,00	"
49 (2-2-68)	"	226,4	302,2	179,0	6,6	9	1,037	7,42	1,05	CENTRAL CELL	0,967	7,42	1,05	"
41 (2-7-69)	"	231,0	281,5	221,6	0,8	9	1,051	2,93	1,03	"	0,950	2,93	1,03	"
16 (2-7-69)	"	227,0	257,5	260,6	- 3,6	2-9	-	-	-	-	0,956	- 1,41	1,01	-
105 (16-7-68)	144	50,2	302,2	99,9	38,9	2-9	0,911 ++	38,38	0,98	SIDE CELL	-	-	-	

\+ Out of range for mass flow rate

++ Out of range for mass flow rate in cold wall correction

TABLE II - (FOLLOWS)

EXPERIMENTAL DATA							ANALYTICAL RESULTS							
Run	Nominal pressure ata	Mass flow rate g/cm²s	Inlet temperature °C	Critical heat flux W/cm²	Average exit quality %	B.O Rods position in the lattice	ΔH-FIAT DNBR	Subchannel local quality %	G out / G in	Subchannel critical heat flux location	W - 3 DNBR	Subchannel local quality %	G out / G in	Subchannel critical heat flux location
65 (16-7-68)	144	50,9	252,7	127,5	31,0	9	0,852	37,41	1,11	CENTRAL CELL	-	-	-	-
16 (19-1-68)	"	93,5	295,0	120,2	14,2	9	0,999	17,05	1,04	"	0,943 +	17,05	1,04	CENTRAL CELL
8 (17-6-68)	"	91,2	285,2	132,4	14,0	2-9	1,026	19,88	1,04	"	-	-	-	-
55 (16-7-68)	"	94,8	254,0	151,7	4,0	2-9	0,922 ++	1,72	1,00	SIDE CELL	1,074 +	8,44	1,04	CENTRAL CELL
25 (19-1-68)	"	158,8	294,3	150,2	4,9	9	1,091	4,79	1,04	CENTRAL CELL	1,139	4,79	1,04	"
50 (16-7-68)	"	151,4	276,2	183,6	2,3	9	1,029	6,39	1,02	"	0,948	8,39	1,02	"
16 (16-7-68)	"	221,4	305,0	165,9	5,8	9	0,949	10,56	1,02	"	0,822	10,56	1,02	"
26 (4-7-69)	158	155,0	309,0	144,0	5,9	9	0,976	5,47	1,04	"	0,962	6,47	1,04	"
14 (4-7-69)	"	155,0	289,0	165,7	- 0,8	9	-	-	-	-	1,070	- 0,21	1,03	"
43 (4-7-69)	"	154,0	240,2	226,6	-12,5	9	-	-	-	-	1,087	-10,53	1,02	"
37 (3-7-69)	"	301,0	322,0	205,2	5,0	9	0,927	5,80	1,04	CENTRAL CELL	0,709	5,80	1,04	"
23 (3-7-69)	"	295,0	311,2	229,0	1,3	9	1,018	1,29	1,04	"	0,794	1,29	1,04	"
56 (3-7-69)	"	297,0	290,7	271,6	- 4,9	9	-	-	-	-	0,876	- 4,99	1,02	"

\+ Out of range for mass flow rate

++ Out of range for mass flow rate in cold wall correction

TABLE III - EXPERIMENTAL DATA AND ANALYTICAL RESULTS FOR CHANNEL B SET. 1

EXPERIMENTAL DATA							ANALYTICAL RESULTS							
Run	Nominal pressure ata	Mass flow rate g/cm²s	Inlet temperature °C	Critical heat flux W/cm²	Average exit quality %	B.O. Rods position in the lattice	ΔH-FIAT DNBR	Subchannel local quality %	G out / G in	Subchannel critical heat flux location	W-3 DNBR	Subchannel local quality %	G out / G in	Subchannel critical heat flux location
85 (21-8-68)	132	50,3	316,5	89,1	41,2	1-2-4-8	0,921 ++	37,02	0,86	CORNER CELL	-	-	-	-
12 (21-8-68)	"	50,3	255,5	128,1	35,7	2-8-9	0,877 ++	32,92	0,99	SIDE CELL	-	-	-	-
19 (21-8-68)	"	50,6	216,5	148,1	30,1	2	0,851 ++	27,22	0,98	SIDE CELL	-	-	-	-
53 (21-8-68)	"	94,5	315,1	112,0	22,7	7	0,978	27,88	1,06	CENTRAL CELL	-	-	-	-
40 (19-8-68)	"	95,8	275,5	150,8	14,5	2-9	0,953 ++	14,79	1,02	SIDE CELL	-	-	-	-
44 (21-8-68)	"	96,4	246,5	171,7	10,2	2	0,939 ++	8,33	0,97	SIDE CELL	0,899 +	16,34	0,95	CENTRAL CELL
90 (9-8-68)	"	161,3	290,0	162,6	6,2	2	1,039	11,05	1,02	CENTRAL CELL	0,934	12,06	0,93	CENTRAL CELL
55 (19-8-68)	"	158,7	275,5	181,7	4,5	2	1,040	3,12	1,02	SIDE CELL	0,981	8,84	0,93	CENTRAL CELL
67 (21-8-68)	"	224,1	312,2	161,0	8,1	9	0,979	12,64	0,94	CENTRAL CELL	0,895	12,64	0,94	CENTRAL CELL
73 (19-8-68)	"	223,9	304,5	184,8	7,25	9	0,954	12,14	0,93	CENTRAL CELL	0,809	12,14	0,93	CENTRAL CELL

\+ Out of range for mass flow rate

++ Out of range for mass flow rate in cold wall correction

TABLE IV - EXPERIMENTAL DATA AND ANALYTICAL RESULTS FOR CHANNEL B SET. II.1

EXPERIMENTAL DATA							ANALYTICAL RESULTS							
Run	Nominal pressure ata	Mass flow rate g/cm^2s	Inlet temperature °C	Critical heat flux W/cm^2	Average exit quality %	B.O. Rods position in the lattice	ΔH-FIAT DNBR	Subchannel local quality %	$\frac{G\,out}{G\,in}$	Subchannel critical heat flux location	W - 3 DNBR	Subchannel local quality %	$\frac{G\,out}{G\,in}$	Subchannel critical heat flux location
62 (20-9-68)	84	52,1	277,0	126,1	42,0	1-2	0,884 ++	38,90	0,96	CORNER CELL	-	-	-	-
77 (20-9-68)	"	52,4	267,5	135,2	42,7	1	0,950 ++	38,74	0,96	"	-	-	-	-
8 (19-8-68)	"	52,3	211,5	163,6	35,5	1	0,890 ++	29,62	0,95	"	-	-	-	-
9 (20-9-68)	"	51,5	184,2	183,5	36,4	1-2	0,838 ++	28,84	0,96	"	-	-	-	-
111 (20-9-68)	"	96,6	285,7	160,6	28,9	1	0,991 ++	27,11	1,00	"	-	-	-	-
70 (20-9-68)	"	97,2	271,0	179,2	28,6	1	0,954 ++	25,11	1,00	"	-	-	-	-
32 (20-9-68)	"	96,6	255,7	192,5	26,2	1	0,934 ++	22,33	1,01	"	-	-	-	-
83 (23-9-68)	132	52,9	311,7	96,4	36,0	1	0,912 ++	33,74	0,91	"	-	-	-	-
74 (12-9-68)	"	50,9	258,5	136,7	34,1	1	0,788 ++	29,16	0,91	"	-	-	-	-
30 (12-9-68)	"	51,9	186,0	175,3	23,1	1-2	0,700 ++	16,22	0,97	"	-	-	-	-
80 (23-9-68)	"	97,3	314,2	115,6	20,9	1	1,003 ++	19,30	0,96	"	-	-	-	-
25 (11-9-68)	"	96,3	280,0	143,0	12,0	1	0,933 ++	9,44	0,99	"	1,193 ++	15,67	0,98	CENTRAL CELL
53 (12-9-68)	"	95,0	242,0	184,2	7,4	1	0,800 ++	3,69	1,01	"	1,062 ++	12,12	0,97	"
9 (23-9-68)	"	159,2	303,3	153,2	8,9	1	1,066	12,07	0,98	CENTRAL CELL	1,084	12,07	0,98	"
52 (11-9-68)	"	163,1	279,1	176,8	1,4	1	1,115	4,12	0,98	"	1,164	4,12	0,98	"

+ Out of range for mass flow rate

++ Out of range for mass flow rate in cold wall correction

TABLE IV - (FOLLOWS)

EXPERIMENTAL DATA							ANALYTICAL RESULTS							
Run	Nominal pressure ata	Mass flow rate g/cm²s	Inlet temperature °C	Critical heat flux W/cm²	Average exit quality %	B.O. Rods position in the lattice	ΔH-FIAT DNBR	Subchannel local quality %	G out / G in	Subchannel critical heat flux location	W-3 DNBR	Subchannel local quality %	G out / G in	Subchannel critical heat flux location
9 (13-9-68)+	132	162,5	247,0	213,4	- 7,2	1	-	-	-	-	1,168	- 3,5	0,98	CENTRAL CELL
63 (23-9-68)	"	240,2	312,0	165,1	6,5	1	1,116	8,74	0,98	CENTRAL CELL	1,042	8,74	0,98	"
54 (23-9-68)+	"	230,9	300,2	188,8	4,8	1	1,092	6,44	0,98	"	0,998	6,44	0,98	"
31 (13-9-68)	"	230,0	285,2	209,8	- 0,8	1	-	-	-	-	1,063	1,04	0,98	"

\+ Out of range for mass flow rate

++ Out of range for mass flow rate in cold wall correction

TABLE V - EXPERIMENTAL DATA AND ANALYTICAL RESULTS FOR CHANNEL B SET. II.2

EXPERIMENTAL DATA							ANALYTICAL RESULTS							
Run	Nominal pressure ata	Mass flow rate $g/cm^2 s$	Inlet temperature °C	Critical heat flux W/cm^2	Average exit quality %	B.O. Rods position in the lattice	ΔH-FIAT DNBR	Subchannel local quality %	G out / G in	Subchannel critical heat flux location	W - 3 DNBR	Subchannel local quality %	G out / G in	Subchannel critical heat flux location
33 (24-10-68)	132	48,3	303,3	102,7	24,0	8	0,962 ++	40,32	0,92	SIDE CELL	-	-	-	-
48 (24-10-68)	"	50,0	284,5	124,5	21,6	8	0,886 ++	41,13	0,91	"	-	-	-	-
59 (24-10-68)	"	51,3	257,2	142,0	17,0	8	0,884 ++	35,83	0,86	"	-	-	-	-
31 (24-10-68)	"	96,0	309,5	133,8	11,0	1	0,998 ++	24,83	0,85	"	-	-	-	-
93 (24-10-68)	"	97,2	296,0	138,7	6,1	1	1,023 ++	12,85	0,85	CORNER CELL	-	-	-	-
75 (24-10-68)	"	95,0	266,2	172,0	1,9	8	0,974 ++	15,21	0,83	SIDE CELL	1,069 ++	8,34	1,03	CENTRAL CELL
16 (24-10-68)	"	164,7	313,7	149,0	5,0	1-8	1,075	10,65	1,01	CENTRAL CELL	1,039	10,65	1,01	"
112 (24-10-68)	"	164,4	309,8	148,3	2,9	1	1,127	8,42	1,02	CENTRAL CELL	1,111	8,42	1,02	"
92 (23-10-68)	"	160,0	284,5	184,5	- 2,9	1	1,051	1,16	0,87	CORNER CELL	1,083	1,75	1,01	"
64 (23-10-68)	"	233,0	311,2	176,5	2,2	1	1,085	5,83	1,03	CENTRAL CELL	0,993	5,83	1,03	"
76 (23-10-68)	"	233,9	290,0	215,2	- 5,8	1-8	-	-	-	-	1,009	2,33	0,84	SIDE CELL
39 (23-10-68)	"	230,3	285,2	217,4	- 7,0	1	-	-	-	-	1,038	0,65	0,83	SIDE CELL
49 (23-10-68)	140	238,1	314,7	162,0	0,5	8	1,148	3,45	1,04	CENTRAL CELL	1,100	3,45	1,04	CENTRAL CELL
10 (25-10-68)	"	225,3	278,7	234,2	-12,5	1	-	-	-	-	0,996	- 2,92	0,85	SIDE CELL
29 (25-10-68)	"	230,0	256,2	266,9	-17,7	1	-	-	-	-	1,033	-10,43	0,87	SIDE CELL

\+ Out of range for mass flow rate

++ Out of range for mass flow rate in cold wall correction

TABLE VI - EXPERIMENTAL DATA AND ANALYTICAL RESULTS FOR CHANNEL B SET. II.3

EXPERIMENTAL DATA							ANALYTICAL RESULTS						
Run	Nominal pressure ata	Mass flow rate g/cm^{2}s	Inlet temperature °C	Critical heat flux W/cm^2	Average exit quality %	B.O. Rods position in the lattice	ΔH-FIAT DNBR	Subchannel local quality %	G out / G in	Subchannel critical heat flux location	W - 3 DNBR	Subchannel local quality %	G out / G in	Subchannel critical heat flux location
33 (16-4-69)	132	93,5	310,5	127,1	7,4	9	1,163 ++	17,18	0,97	CENTRAL CELL	1,117 ++	17,18	0,97	CENTRAL CELL
46 (16-4-69)	"	93,0	240,5	205,5	-11,1	9	-	-	-	-	1,014 ++	2,65	0,95	"
65 (16-4-69)	"	93,0	204,0	237,9	-21,7	9	-	-	-	-	1,028 ++	- 5,90	0,96	"
10 (2-4-69)	"	157,0	308,5	148,5	- 0,1	9	1,228	7,35	0,97	CENTRAL CELL	1,142	7,35	0,97	"
21 (24-3-69)	"	153,4	287,8	169,3	- 6,4	9	-	-	-	-	1,198	0,28	0,97	"
9 (26-3-69)	"	156,0	240,5	223,7	-22,5	9	-	-	-	-	1,269	-14,26	1,05	"
30 (25-3-69)	"	156,6	202,5	222,7	-33,9	9	-	-	-	-	1,195	-24,45	1,05	"
65 (31-3-69)	"	225,6	306,8	180,7	- 2,2	9	1,205	3,54	0,97	CENTRAL CELL	1,036	3,54	0,97	"
37 (27-3-69)	"	224,9	282,0	224,2	-10,8	9	-	-	-	-	1,067	- 4,85	0,98	"
59 (27-3-69)	"	224,8	262,0	248,0	-18,1	9	-	-	-	-	1,167	-11,77	0,97	"
14 (1-4-69)	"	224,8	241,9	285,7	-24,0	9	-	-	-	-	1,129	-16,87	1,04	"
9 (10-4-69)	158	156,0	319,7	140,3	- 3,1	9	1,116	3,80	0,99	CENTRAL CELL	1,071	3,80	0,99	"
52 (11-4-69)	"	156,3	270,2	194,9	-24,1	9	-	-	-	-	1,136	-14,25	1,03	"
26 (11-4-69)	"	155,6	243,7	226,8	-33,9	9	-	-	-	-	1,146	-24,38	1,05	"
41 (11-4-69)	"	155,9	203,2	267,0	-47,3	9	-	-	-	-	1,046	-37,33	1,05	"

\+ Out of range for mass flow rate

++ Out of range for mass flow rate in cold wall correction

TABLE VI - (FOLLOWS)

EXPERIMENTAL DATA							ANALYTICAL RESULTS							
Run	Nominal pressure ata	Mass flow rate g/cm²s	Inlet temperature °C	Critical heat flux W/cm²	Average exit quality %	B.O Rods position in the lattice	ΔH-FIAT DNBR	Subchannel local quality %	G out / G in	Subchannel critical heat flux location	W-3 DNBR	Subchannel local quality %	G out / G in	Subchannel critical heat flux location
21 (2-4-69)	158	297,8	320,8	211,3	- 5,8	9	-	-	-	-	0,843	- 0,11	0,99	CENTRAL CELL
26 (2-4-69)	"	300,9	309,1	247,4	- 10,3	9	-	-	-	-	0,847	- 4,68	0,99	"
54 (2-4-69)	"	298,7	294,9	294,7	- 16,0	9	-	-	-	-	0,790	- 8,93	0,99	"

\+ Out of range for mass flow rate

++ Out of range for mass flow rate in cold wall correction

TABLE VIII - EXPERIMENTAL DATA AND ANALYTICAL RESULTS FOR CHANNEL B SET. II.4

	EXPERIMENTAL DATA						ANALYTICAL RESULTS							
Run	Nominal pressure ata	Mass flow rate $g/cm^2 s$	Inlet temperature °C	Critical heat flux W/cm^2	Average exit quality %	B.O. Rods position in the lattice	ΔH-FIAT DNBR	Subchannel local quality %	$\frac{G\ out}{G\ in}$	Subchannel critical heat flux location	W-3 DNBR	Subchannel local quality %	$\frac{G\ out}{G\ in}$	Subchannel critical heat flux location
76 (26-11-68)	84	51,5	293,0	130,6	27,0	9	1,355 ++	49,54	0,92	CENTRAL CELL	-	-	-	-
34 (26-11-68)	"	50,8	267,2	161,1	26,2	9	1,185 ++	53,01	0,93	"	-	-	-	-
40 (26-11-68)	"	51,3	222,7	198,4	24,5	9	1,082 ++	54,76	0,88	"	-	-	-	-
84 (26-11-68)	"	96,8	286,5	164,6	14,6	9	1,353 ++	31,84	0,81	"	-	-	-	-
16 (26-11-68)	"	96,5	257,5	194,4	9,5	9	1,313 ++	29,41	0,75	"	-	-	-	-
52 (26-11-68)	"	93,3	227,7	227,4	5,3	9	1,243 ++	29,1	0,73	"	-	-	-	-
122 (25-11-68)	132	51,9	309,1	106,7	18,2	9	1,059 ++	38,23	0,97	"	-	-	-	-
29 (22-11-68)	"	51,0	261,7	141,1	5,8	9	1,015 ++	32,51	0,93	"	-	-	-	-
30 (25-11-68)	"	51,2	223,0	179,6	1,4	9	0,918 ++	34,36	0,91	"	-	-	-	-
113 (25-11-68)	"	97,7	310,7	117,9	5,5	9	1,243 ++	18,86	0,87	"	-	-	-	-
12 (22-11-68)	"	95,1	280,7	142,7	- 4,8	9	1,230 ++	10,95	0,87	"	1,310 ++	10,95	0,87	CENTRAL CELL
10 (25-11-68)	"	101,2	223,2	194,4	- 22,2	9	-	-	-	-	1,287 ++	- 4,60	0,88	"
87 (25-11-68)	"	157,2	301,5	157,2	- 2,7	9	1,251	8,93	0,85	CENTRAL CELL	1,146	8,93	0,85	"
128 (25-11-68)	"	155,6	275,0	188,6	- 9,4	9	1,248	13,69	0,85	"	1,147	13,69	0,85	"
42 (25-11-68)	"	157,1	243,7	224,5	- 21,2	9	-	-	-	-	1,170	- 7,67	0,88	"

\+ Out of range for mass flow rate

++ Out of range for mass flow rate in cold wall correction

TABLE VII - (FOLLOWS)

EXPERIMENTAL DATA							ANALYTICAL RESULTS							
Run	Nominal pressure ata	Mass flow rate $g/cm^2 s$	Inlet temperature °C	Critical heat flux W/cm^2	Average exit quality %	B.O. Rods position in the lattice	ΔH-FIAT DNBR	Subchannel local quality %	$\frac{G_{out}}{G_{in}}$	Subchannel critical heat flux location	W-3 DNBR	Subchannel local quality %	$\frac{G_{out}}{G_{in}}$	Subchannel critical heat flux location
97 (25-11-68)	132	234,9	311,7	157,2	- 1,8	9	-	-	-	-	1,191	5,63	0,88	CENTRAL CELL
93 (25-11-68)	"	226,4	299,7	179,9	- 6,1	9	-	-	-	-	1,146	2,54	0,87	"
61 (22-11-68)	"	223,2	279,4	207,1	- 12,3	9	-	-	-	-	1,188	- 4,11	0,88	"

\+ Out of range for mass flow rate

++ Out of range for mass flow rate in cold wall correction

TABLE VIII - EXPERIMENTAL DATA AND ANALYTICAL RESULTS FOR CHANNEL B SET. II.5

EXPERIMENTAL DATA							ANALYTICAL RESULTS							
Run	Nominal pressure ata	Mass flow rate g/cm²s	Inlet temperature °C	Critical heat flux W/cm²	Average exit quality %	B.O. Rods position in the lattice	ΔH-FIAT DNBR	Subchannel local quality %	G out / G in	Subchannel critical heat flux location	W - 3 DNBR	Subchannel local quality %	G out / G in	Subchannel critical heat flux location
130 (16-12-68)	84	51,2	290,5	129,3	40,2	8	1,236 ++	43,57	0,98	SIDE CELL	-	-	-	-
120 (16-12-68)	"	51,1	264,0	146,9	37,0	8	1,175 ++	40,70	0,98	"	-	-	-	-
94 (16-12-68)	"	52,5	242,2	160,6	33,0	8	1,150 ++	36,91	0,97	"	-	-	-	-
111 (16-12-68)	"	51,5	220,2	176,6	31,6	9-8	1,096 ++	37,09	0,96	"	-	-	-	-
135 (16-12-68)	"	98,0	285,2	170,8	24,7	8	1,194 ++	27,02	0,97	"	-	-	-	-
142 (16-12-68)	"	97,5	277,2	179,5	23,1	8	1,176 ++	26,25	0,97	"	-	-	-	-
22 (16-12-68)	132	51,3	300,7	109,6	28,5	9-8	1,021 ++	33,10	0,96	"	-	-	-	-
21 (13-12-68)	"	51,1	260,5	134,5	22,1	9-8	0,982 ++	26,11	0,92	"	-	-	-	-
41 (13-12-68)	"	52,2	219,0	162,1	14,7	9-8	0,930 ++	19,66	0,90	"	-	-	-	-
33 (16-12-68)	"	97,1	318,0	117,4	17,3	9-8	1,108	24,27	1,02	CENTRAL CELL	-	-	-	-
62 (13-12-68)	"	95,9	280,2	153,2	8,0	9	1,164	15,92	0,97	"	0,962 +	15,92	0,97	CENTRAL CELL
7 (13-12-68)	"	95,7	259,1	174,7	5,4	9	1,155	12,55	0,96	"	0,960 +	12,55	0,96	"
39 (16-12-68)	"	161,1	319,0	129,0	8,4	9	1,176	14,18	1,01	"	1,064	14,18	1,01	"
59 (16-12-68)	"	161,4	307,5	142,4	5,3	9	1,254	10,10	0,99	"	1,126	10,10	0,99	"
69 (13-12-68)	"	157,1	305,0	175,0	- 0,5	9	1,233	5,69	0,99	"	1,069	5,69	0,99	"

\+ Out of range for mass flow rate

++ Out of range for mass flow rate in cold wall correction

TABLE VIII - (FOLLOWS)

EXPERIMENTAL DATA							ANALYTICAL RESULTS							
Run	Nominal pressure ata	Mass flow rate $g/cm^2 s$	Inlet temperature °C	Critical heat flux W/cm^2	Average exit quality %	B.O. Rods position in the lattice	ΔH-FIAT DNBR	Subchannel local quality %	$\frac{G_{out}}{G_{in}}$	Subchannel critical heat flux location	W-3 DNBR	Subchannel local quality %	$\frac{G_{out}}{G_{in}}$	Subchannel critical heat flux location
69 (16-12-68)	132	235,0	315,3	155,8	3,6	9	1,202	8,42	0,99	CENTRAL CELL	1,069	8,42	0,99	CENTRAL CELL
81 (16-12-68)	"	229,4	313,0	167,4	2,8	9	1,150	8,98	0,99	"	0,980	8,98	0,99	"
86 (13-12-68)	"	227,1	305,0	175,0	- 0,5	9	1,229	5,8	0,99	"	1,065	5,80	0,99	"

\+ Out of range for mass flow rate

++ Out of range for mass flow rate in cold wall correction

TABLE IX - EXPERIMENTAL DATA AND ANALYTICAL RESULTS FOR CHANNEL B SET. III

EXPERIMENTAL DATA							ANALYTICAL RESULTS							
Run	Nominal pressure ata	Mass flow rate $g/cm^2 s$	Inlet temperature °C	Critical heat flux W/cm^2	Average exit quality %	B.O. axial position on the central rod (z/l)	ΔH-FIAT DNBR	Subchannel local quality %	$\frac{G_{out}}{G_{in}}$	B.O. axial position on the central cell (z/l)	W - 3 DNBR	Subchannel local quality %	$\frac{G_{out}}{G_{in}}$	B.O. axial position on the central cell (z/l)
7 (3-10-69)	84	48,5	288,5	119,2	27,7	0,70-0,94-- 0,98	1,419 ++	46,79	0,96	1	-	-	-	-
43 (2-10-69)	"	48,7	280,2	125,3	26,2	0,94-0,98	1,390 ++	45,40	0,97	1	-	-	-	-
38 (2-10-69)	"	48,2	271,2	127,7	23,6	0,66-0,94-- 0,98	1,360 ++	44,0	0,98	1	-	-	-	-
32 (2-10-69)	"	49,5	259,6	135,3	21,1	0,66	1,340 ++	42,45	0,98	1	-	-	-	-
25 (2-10-69)	"	48,8	240,0	144,5	17,5	0,66	1,310 ++	40,20	0,98	1	-	-	-	-
21 (2-10-69)	"	49,6	220,0	152,2	12,1	0,66-0,84	1,320 ++	35,70	0,98	1	-	-	-	-
51 (2-10-69)	"	50,8	200,2	164,1	7,8	0,66	1,280 ++	33,10	0,97	1	-	-	-	-
14 (2-10-69)	"	49,4	200,0	155,6	5,2	0,52	1,337 ++	30,60	1,00	1	-	-	-	-
56 (2-10-69)	"	49,5	189,7	169,9	7,3	0,56-0,66	1,255 ++	33,80	0,99	1	-	-	-	-
10 (22-9-69)	132 +	47,2	320,7	71,5	17,2	0,86	1,351 ++	31,72	0,99	1	-	-	-	-
5 (22-9-69)	"	47,5	311,2	74,1	12,8	0,86	1,405 ++	26,87	0,99	1	-	-	-	-
17 (3-10-69)	"	47,4	297,7	90,2	11,8	0,66-0,84--0,94-0,98	1,237 ++	28,61	0,99	1	-	-	-	-
32 (19-9-69)	"	48,5	288,5	91,7	7,3	0,69-0,86	1,293 ++	23,5	0,98	1	-	-	-	-
26 (19-9-69)	"	46,2	270,5	101,3	3,5	0,86-0,94	-	-	-	-	1,230 ++	6,34	1,00	0,61
18 (19-9-69)	"	47,6	249,0	110,3	- 2,8	0,6-0,69-- 0,81	-	-	-	-	1,246 ++	- 1,32	1,02	0,61

\+ Out of range for mass flow rate

++ Out of range for mass flow rate in cold wall correction

TABLE IX (FOLLOWS)

EXPERIMENTAL DATA							ANALYTICAL RESULTS							
Run	Nominal pressure ata	Mass flow rate g/cm²s	Inlet temperature °C	Critical heat flux W/cm²	Average exit quality %	B.O. axial position on the central rod (z/l)	ΔH-FIAT DNBR	Subchannel local quality %	G out / G in	B.O. axial position on the central cell (z/l)	W - 3 DNBR	Subchannel local quality %	G out / G in	B.O. axial position on the central cell (z/l)
11 (19-9-69)	132	48,2	241,7	117,2	- 2,5	0,69-0,81-- 0,9	-	-	-	-	1,198 ++	- 2,52	1,01	0,61
24 (3-10-69)	"	49,9	231,7	135,8	- 3,0	0,58-0,66- 0,56	-	-	-	-	1,038 ++	- 0,96	1,00	0,61
16 (22-9-69)	"	49,0	219,7	136,5	- 6,4	0,5	-	-	-	-	1,088 ++	- 5,55	0,99	0,61
29 (3-10-69)	"	50,3	199,5	145,1	-13,1	0,52	-	-	-	-	1,076 ++	- 21,69	1,01	0,61
13 (9-10-69)	"	94,4	308,0	91,3	1,8	0,94-0,98	-	-	-	-	1,283 ++	3,59	1,10	0,61
6 (9-10-69)	"	91,3	300,0	96,0	- 1,0	0,94-0,98	-	-	-	-	1,249 ++	- 3,61	1,10	0,57
28 (8-10-69)	"	94,4	282,2	116,3	- 5,6	0,94	-	-	-	-	1,154 ++	- 9,87	1,08	0,57
33 (9-10-69)	"	93,0	261,7	124,0	-13,5	0,8-0,89	-	-	-	-	1,202 ++	- 17,94	1,09	0,57
21 (8-10-69)	"	95,2	257,2	133,7	-14,2	0,89	-	-	-	-	1,128 ++	- 18,97	1,09	0,57
14 (21-10-69)	"	93,6	248,2	134,5	-17,0	0,7-0,75	-	-	-	-	1,135 ++	- 24,23	1,16	0,54
7 (8-10-69)	"	93,9	235,2	146,9	-20,3	0,52	-	-	-	-	1,058 ++	- 28,24	1,16	0,54
14 (8-10-69)	"	93,1	220,7	160,1	-23,7	0,52-0,66--0,8-0,89	-	-	-	-	0,979 ++	- 35,19	1,15	0,54
4 (10-10-69)	"	92,9	212,2	150,4	-28,7	0,61-0,66--0,7-0,75	-	-	-	-	1,040 ++	- 39,65	1,15	0,54
3 (21-10-69)	"	92,0	210,5	153,3	-29,1	0,61-0,66-0,7	-	-	-	-	1,020 ++	- 39,8	1,15	0,54
24 (9-10-69)	"	93,0	201,0	162,2	-31,0	0,52-0,56--0,8-0,89	-	-	-	-	0,968 ++	- 42,9	1,15	0,54

\+ Out of range for mass flow rate

++ Out of range for mass flow rate in cold wall correction

TABLE IX (FOLLOWS)

EXPERIMENTAL DATA							ANALYTICAL RESULTS								
Run	Nominal pressure ata	Mass flow rate $g/cm^2 s$	Inlet temperature °C	Critical heat flux W/cm^2	Average exit quality %	B.O. axial position on the central rod (z/l)	ΔH-FIAT DNBR	Subchannel local quality %	$\frac{G\ out}{G\ in}$	B.O. axial position on the central cell (z/l)	W - 3 DNBR	Subchannel local quality %	$\frac{G\ out}{G\ in}$	B.O. axial position on the central cell (z/l)
6 (11-11-69)	132	152,4	311,5	118,7	0,17	0,66	-	-	-	-	0,999	0,15	1,07	0,61
11 (11-11-69)	"	156,9	301,2	131,9	- 2,3	0,66-0,75-- 0,8	-	-	-	-	0,993	- 1,63	0,92	0,61
31 (21-10-69)	"	163,1	295,2	135,8	- 6,1	0,75-0,8--0,84-0,9	-	-	-	-	1,031	- 4,89	0,90	0,61
12 (22-10-69)	"	160,6	287,4	143,0	- 9,6	0,7-0,75--0,8-0,84	-	-	-	-	1,044	- 9,18	0,89	0,57
15 (11-11-69)	"	161,0	280,0	151,5	-10,2	0,66-0,75	-	-	-	-	1,035	- 10,46	0,89	0,61
5 (22-10-69)	"	157,8	266,0	162,2	-16,5	0,7-0,75	-	-	-	-	1,030	- 11,94	1,11	0,57
22 (21-10-69)	"	161,5	258,5	170,1	-18,9	0,52	-	-	-	-	1,018	- 22,33	1,11	0,57
21 (11-11-69)	"	153,6	248,7	182,8	-20,8	0,61-0,66	-	-	-	-	0,954	- 24,75	1,12	0,57
27 (26-11-69)	"	216,1	314,0	130,3	- 1,4	0,66	-	-	-	-	1,026	- 9,23	0,91	0,61
23 (26-11-69)	"	217,8	307,2	140,3	- 3,9	0,66	-	-	-	-	0,984	- 1,19	0,92	0,64
14 (26-11-69)	"	216,9	300,2	146,1	- 6,4	0,66	-	-	-	-	1,009	- 4,24	0,90	0,64
9 (26-11-69)	"	216,5	290,5	159,6	-10,3	0,66	-	-	-	-	1,002	- 7,92	0,89	0,61
6 (26-11-69)	"	225,8	279,0	181,7	-14,0	0,66	-	-	-	-	0,987	- 13,13	0,90	0,61
10 (28-11-69)	"	220,9	271,5	193,9	-16,6	0,66	-	-	-	-	0,957	- 16,58	0,96	0,57
17 (28-11-69)	"	225,3	261,7	204,4	-20,4	0,66	-	-	-	-	0,948	- 20,46	0,97	0,57

\+ Out of range for mass flow rate

++ Out of range for mass flow rate in cold wall correction

TABLE IX (FOLLOWS)

EXPERIMENTAL DATA							ANALYTICAL RESULTS							
Run	Nominal pressure ata	Mass flow rate g/cm^2s	Inlet temperature °C	Critical heat flux W/cm^2	Average exit quality %	B.O. axial position on the central rod (z/l)	ΔH-FIAT DNBR	Subchannel local quality %	$\frac{G_{out}}{G_{in}}$	B.O. axial position on the central cell (z/l)	W - 3 DNBR	Subchannel local quality %	$\frac{G_{out}}{G_{in}}$	B.O. axial position on the central cell (z/l)
17 (20-11-69)	158	157,6	318,0	117,8	- 5,5	0,66	-	-	-	-	0,970	- 4,25	0,92	0,61
12 (22-10-69)	"	155,9	310,0	126,1	- 8,7	0,66	-	-	-	-	0,980	- 8,41	0,91	0,61
3 (20-11-69)	"	152,7	301,5	133,2	- 10,9	0,66	-	-	-	-	0,999	- 12,22	0,91	0,61
3 (21-11-69)	"	155,4	297,2	139,0	- 12,6	0,66	-	-	-	-	0,988	- 18,5	1,11	0,57
13 (27-11-69)	"	156,4	290,0	142,7	- 14,5	0,66	-	-	-	-	0,993	- 22,25	1,12	0,57
9 (27-11-69)	"	157,2	278,5	153,3	- 20,3	0,66	-	-	-	-	0,962	- 27,52	1,12	0,57
4 (28-11-69)	"	302,8	328,2	138,7	- 4,0	0,66	-	-	-	-	0,933	- 2,42	0,93	0,68
7 (27-11-69)	"	299,3	320,7	158,8	- 7,7	0,66	-	-	-	-	0,883	- 5,73	0,92	0,68
3 (27-11-69)	"	297,4	310,0	171,5	- 12,8	0,66	-	-	-	-	0,944	- 12,19	0,92	0,64
8 (27-11-69)	"	298,5	301,7	184,6	- 12,6	0,66	-	-	-	-	0,943	- 17,1	0,92	0,61

\+ Out of range for mass flow rate

++ Out of range for mass flow rate in cold wall correction

F I G U R E S

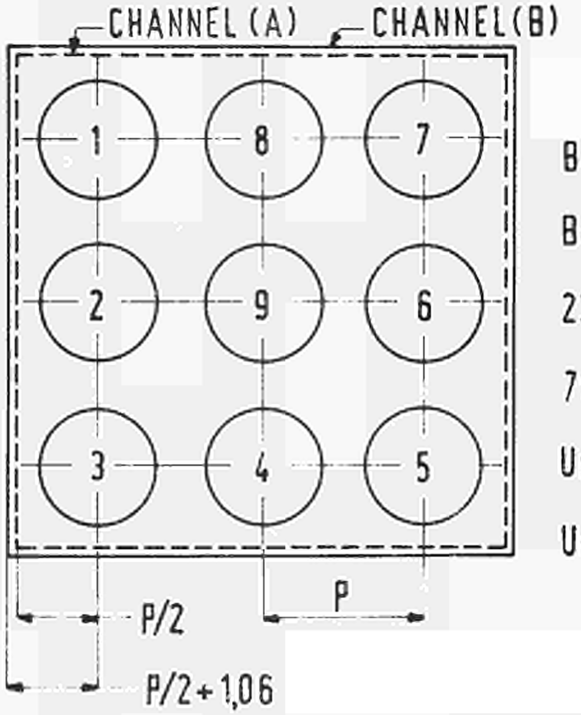

ROD SPECIFICATION		SYMBOLS
Base Load	Axially Uniform	○
Base Load	Axially Non Unif.	⊘
23% Overload	Axially Uniform	(23)
70% Overload	Axially Uniform	(70)
Unheated		●
Unheated	Cluster Control	◉

CHANNEL TYPE AND SET, N°	ROD POSITION IN THE LATTICE								
	1	2	3	4	5	6	7	8	9
A-SET. 0 □	○	○	○	○	○	○	○	○	○
B-SET. 0 ■	○	○	○	○	○	○	○	○	○
B-SET I (•) △	○	○	○	○	○	○	○	○	○
B-SET II.1 ▲	○	○	○	○	○	○	○	○	◉
B-SET II.2 ◇	○	●	○	●	○	●	○	○	○
B-SET II.3 ◆	●	○	●	(23)	●	(23)	●	○	(23)
B-SET II.4 ⬟	●	○	●	(23)	◉	(23)	●	○	(23)
B-SET II.5 ○	○	○	○	(70)	(23)	(23)	(23)	(70)	(70)
B-SET III ●	●	⊘	●	⊘	◉	⊘	●	⊘	⊘

(•)Channel with obstruction in the flow area

Fig. 1 - Nine rods DNB test section. Experimental program index.

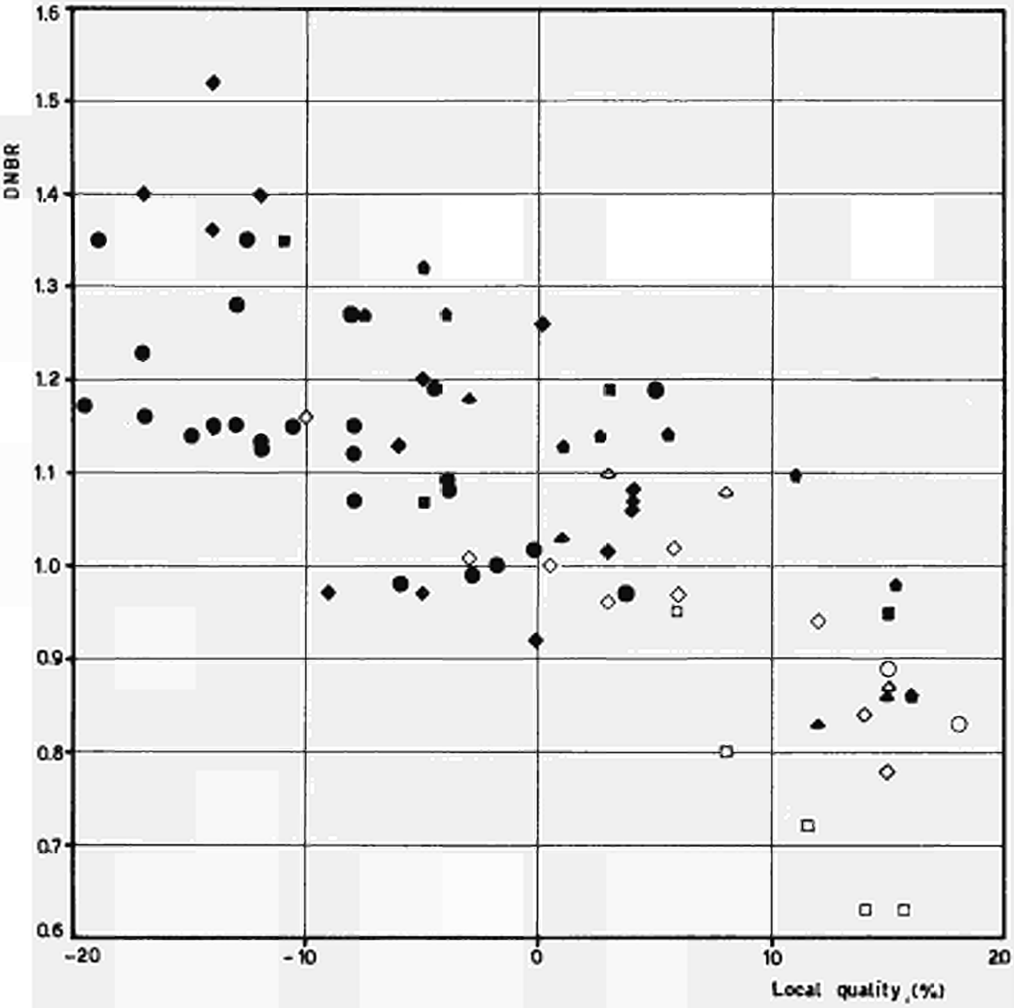

Fig. 2 - DNB Ratios according to W-3 correlation in subchannels with cold wall correction (Ref. 5) for various tests.

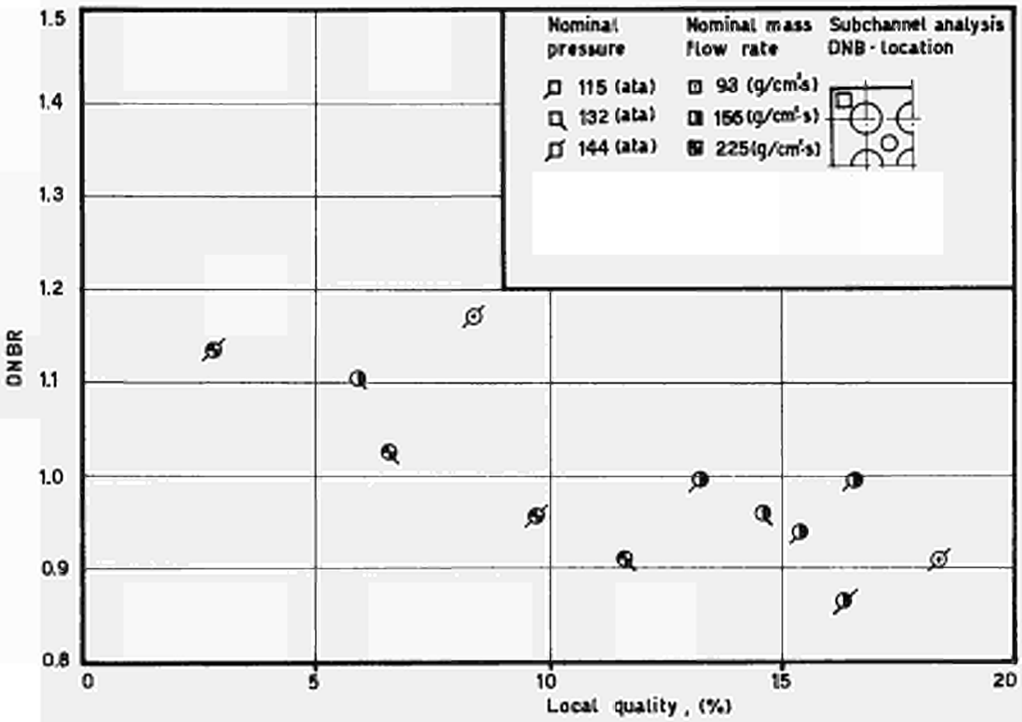

Fig. 3 - DNB Ratios according to W-3 correlation for channel A set O.

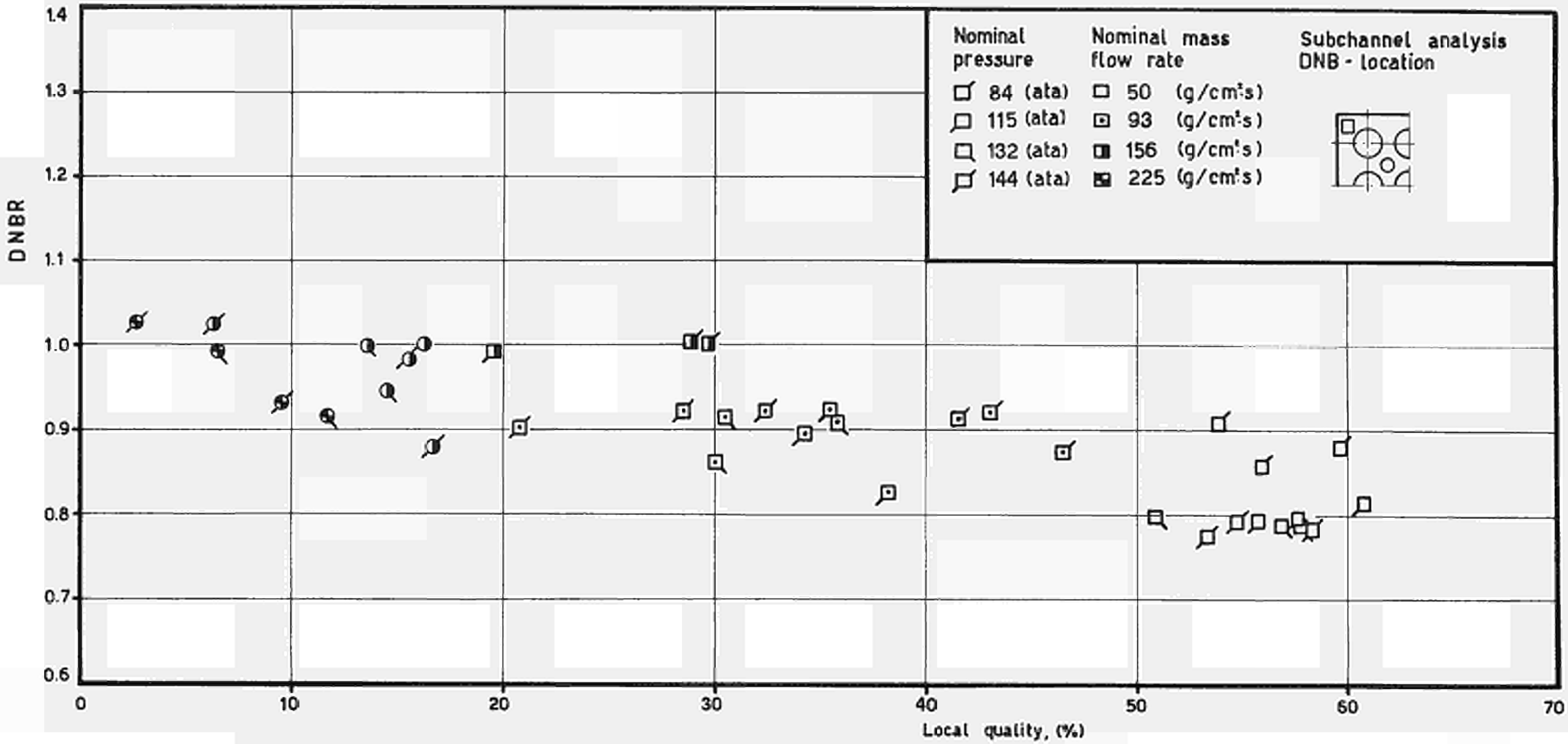

Fig. 4 - DNB Ratios according to ΔH-FIAT correlation for channel A set 0.

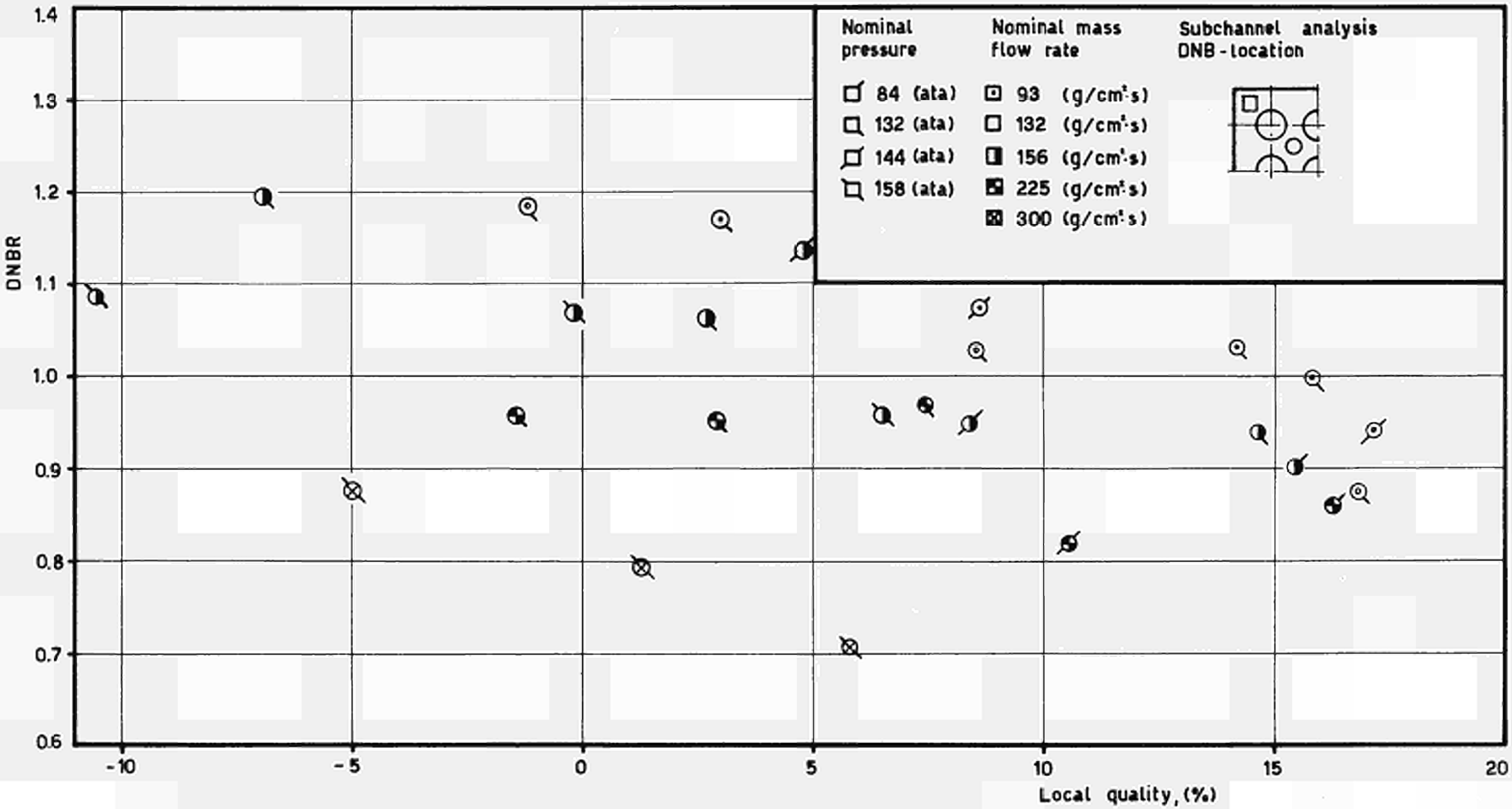

Fig. 5 – DNB Ratios according to W-3 correlation for channel B set O.

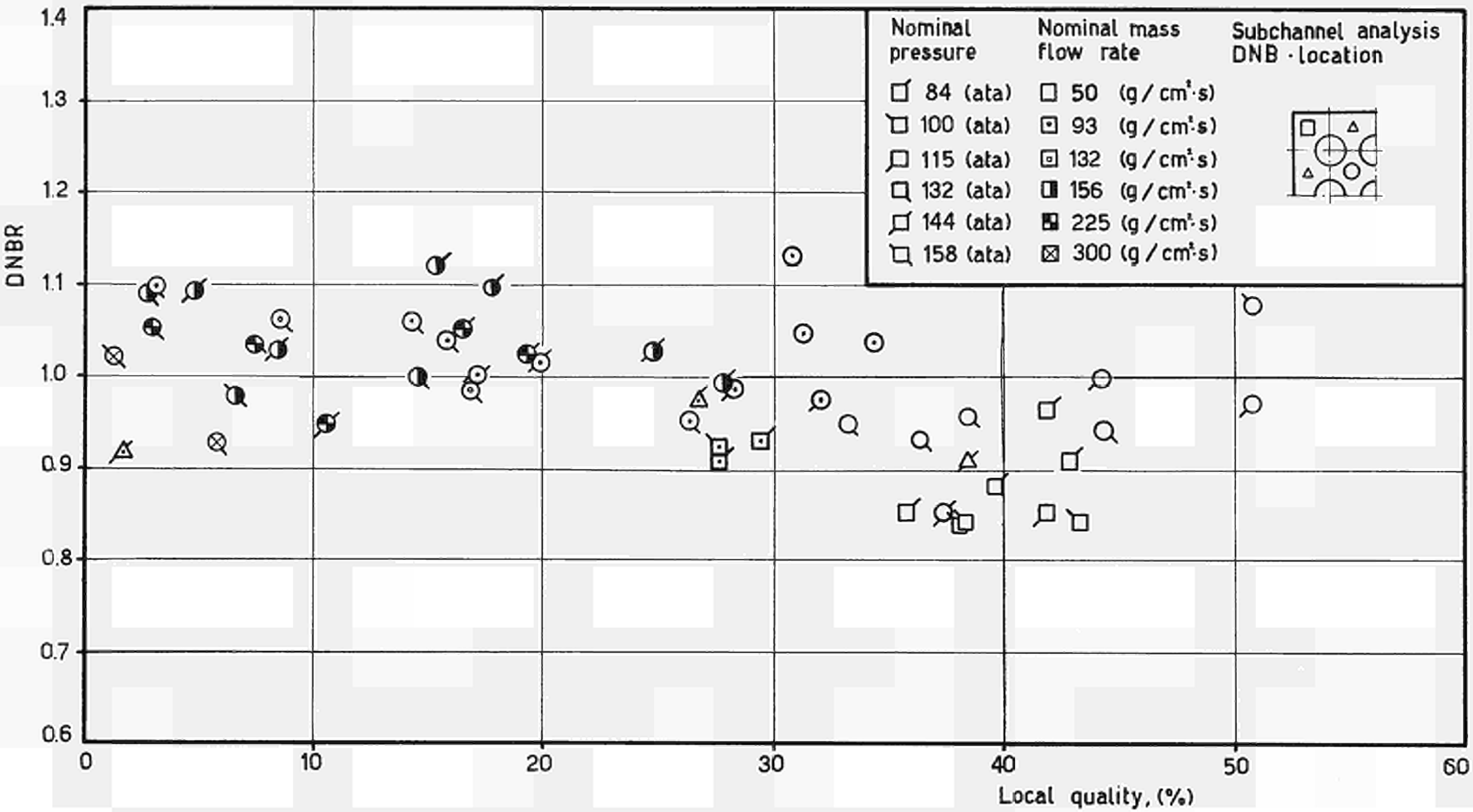

Fig. 6 - DNB Ratios according to △H-FIAT correlation for channel B set O.

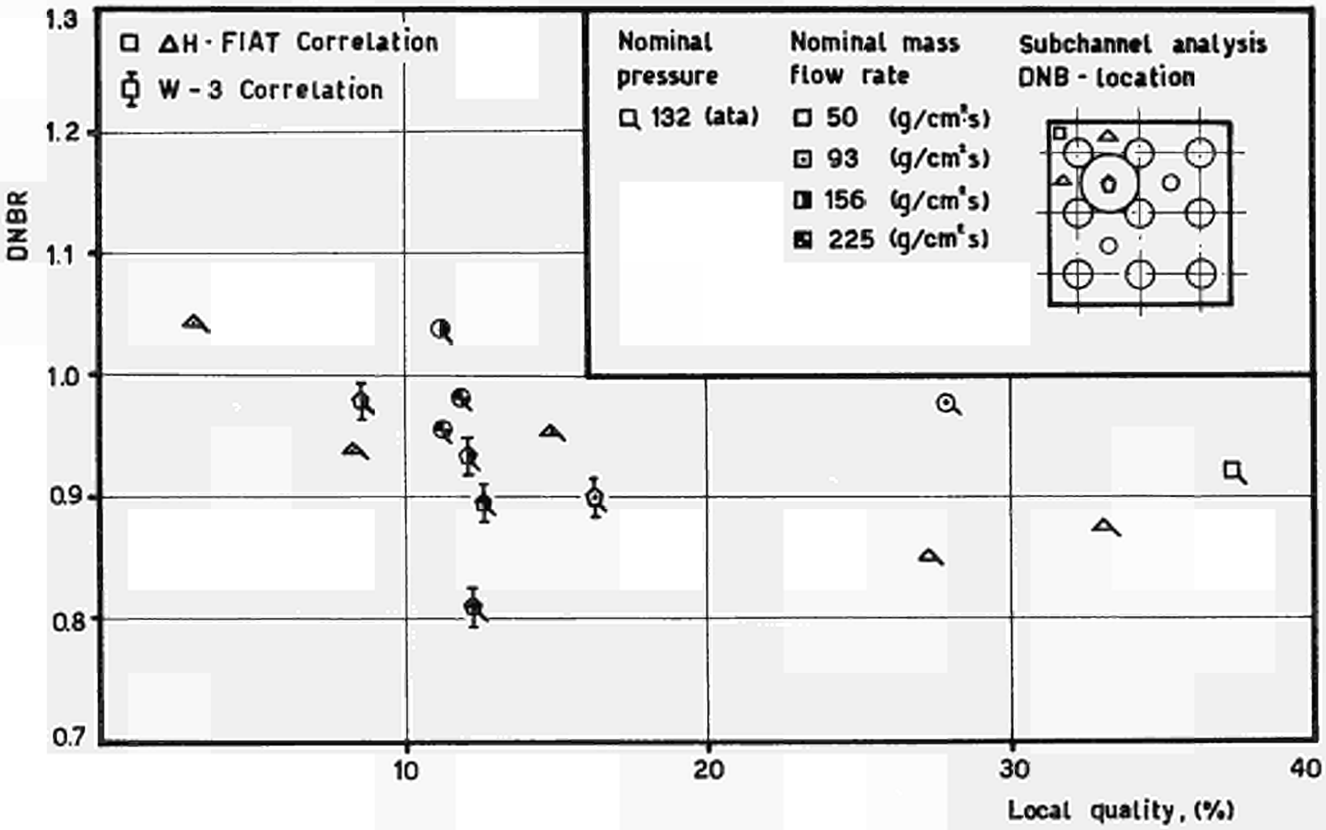

Fig. 7 - DNB Ratios according to ΔH-FIAT and W-3 correlations for channel B set I.

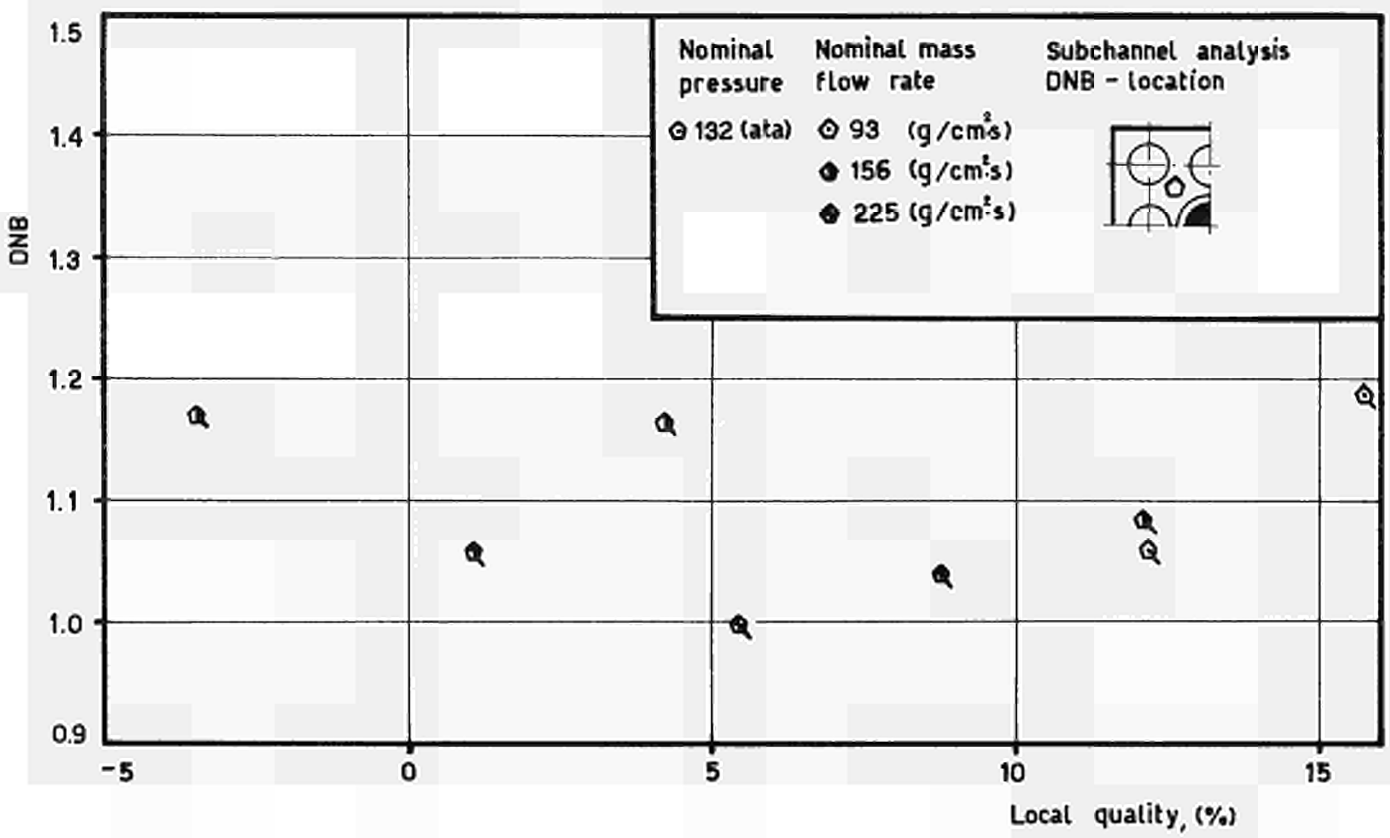

Fig. 8 - DNB Ratios according to W-3 correlation for channel B set II.1

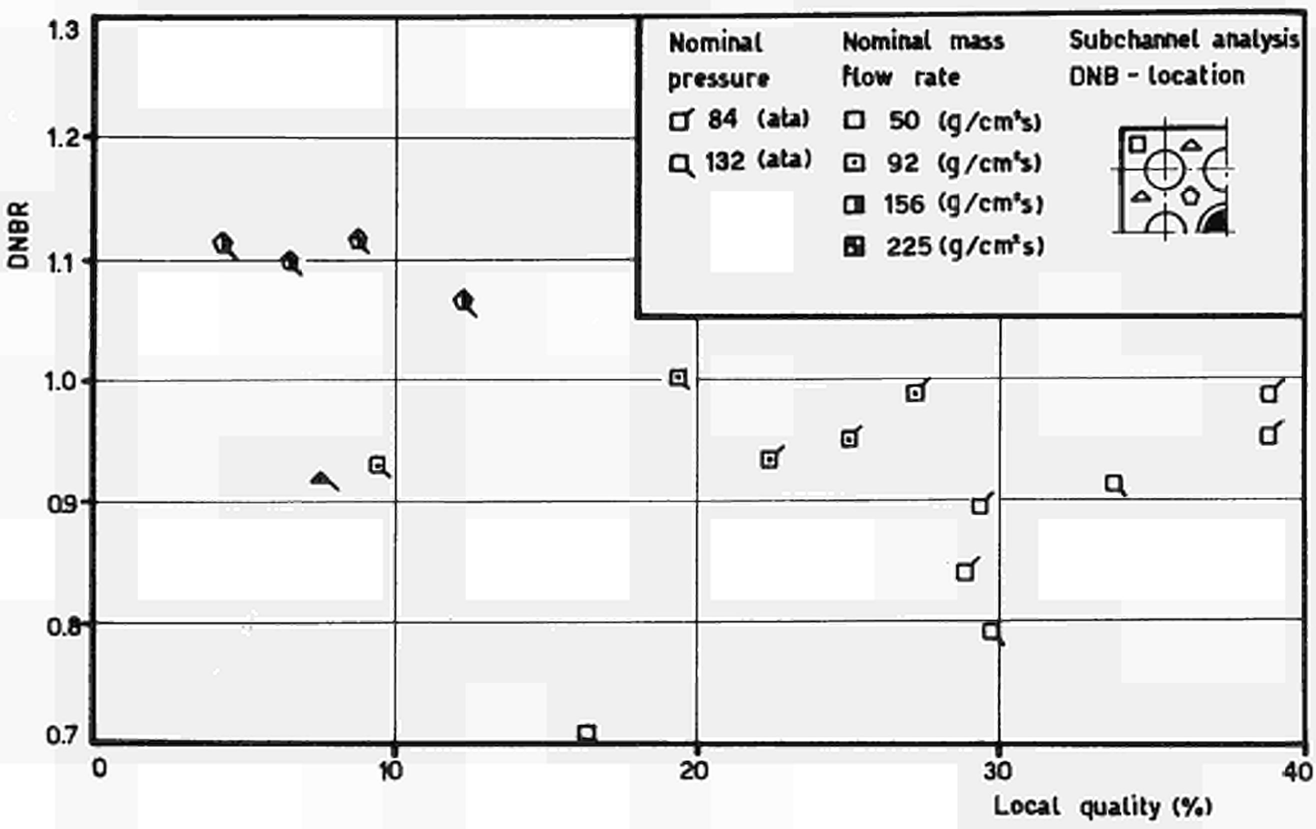

Fig. 9 - DNB Ratios according to ΔH-FIAT correlation for channel B set II.1

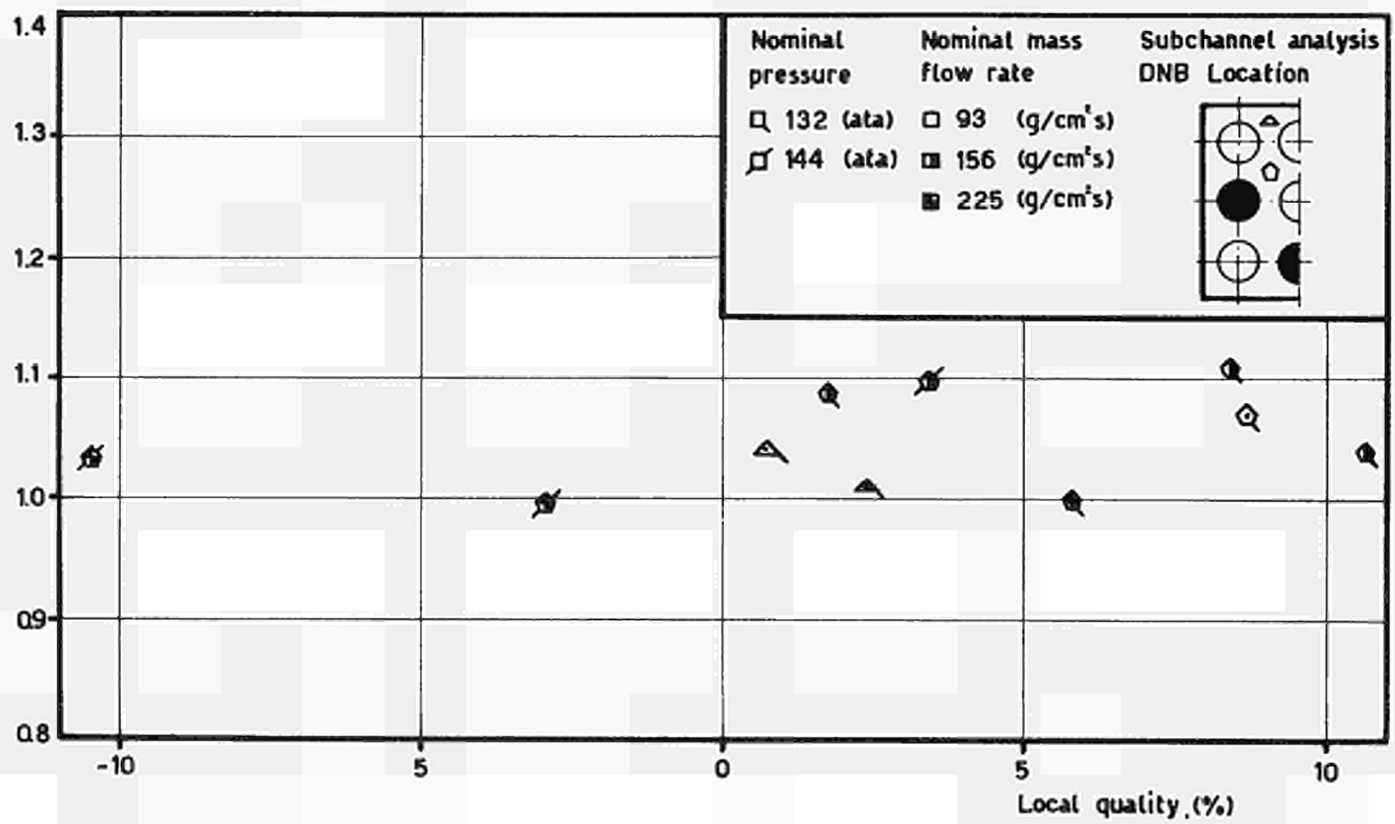

Fig. 10 - DNB Ratios according to W-3 correlation for channel B set II.2

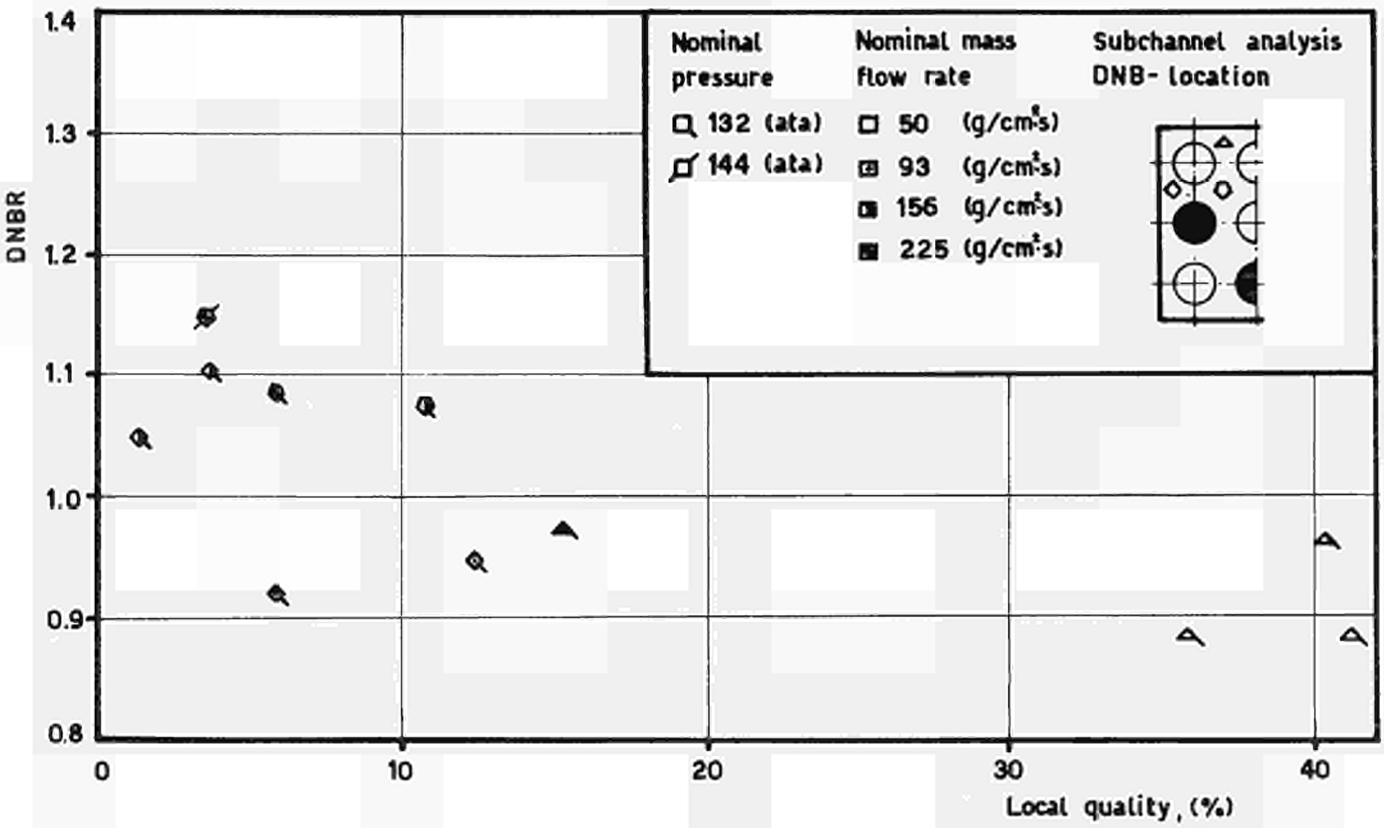

Fig. 11 - DNB Ratios according to △H-FIAT correlation for channel B set II.2

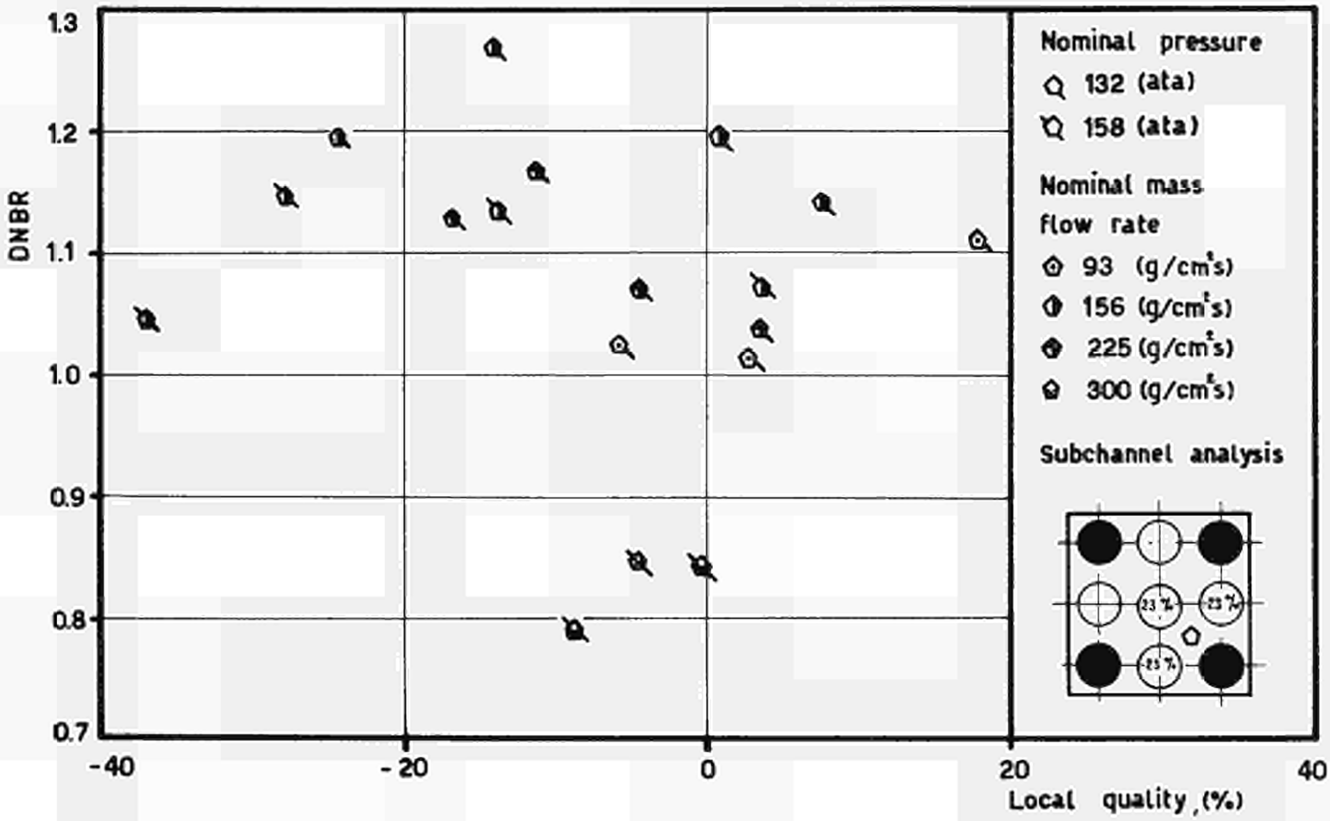

Fig. 12 - DNB Ratios according to W-3 correlation for channel B set II.3

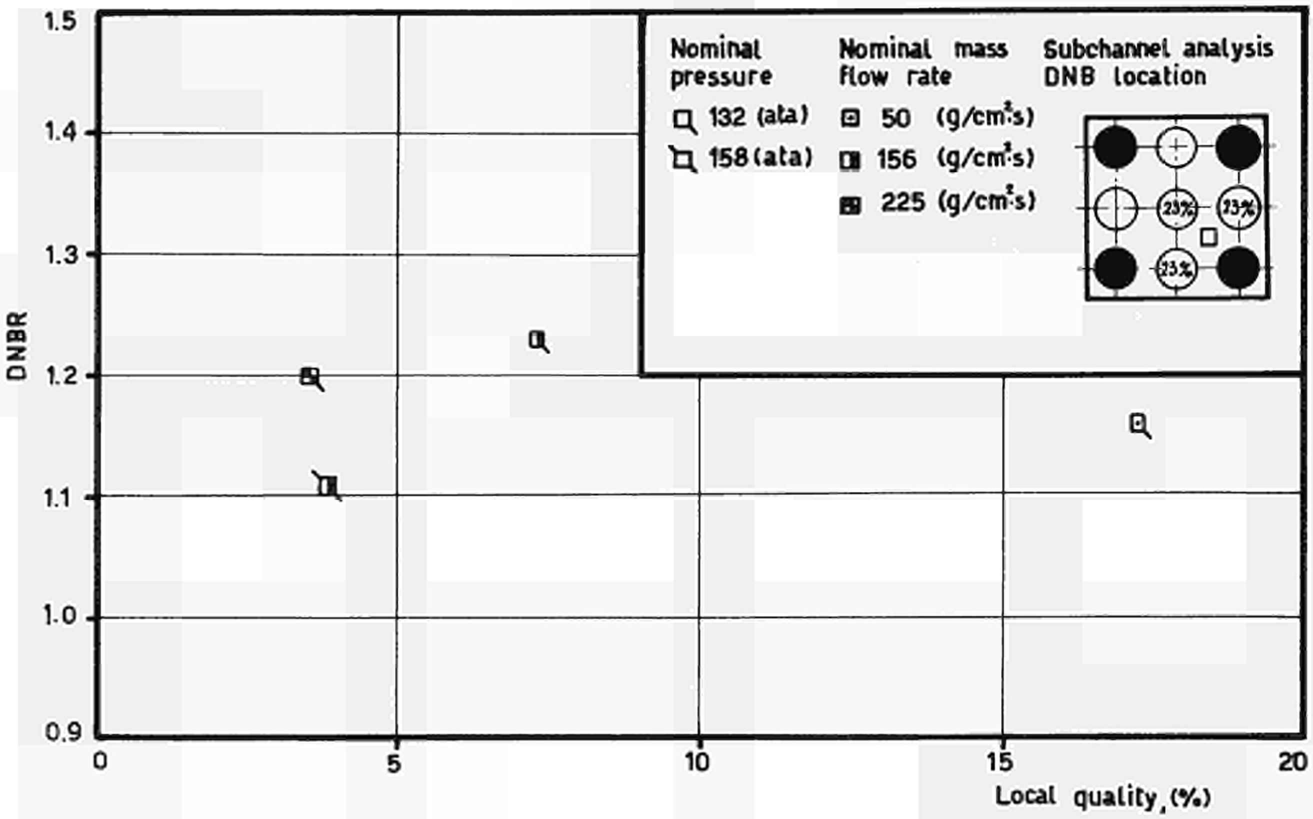

Fig. 13 - DNB Ratios according to △H-FIAT correlation for channel B set II.3

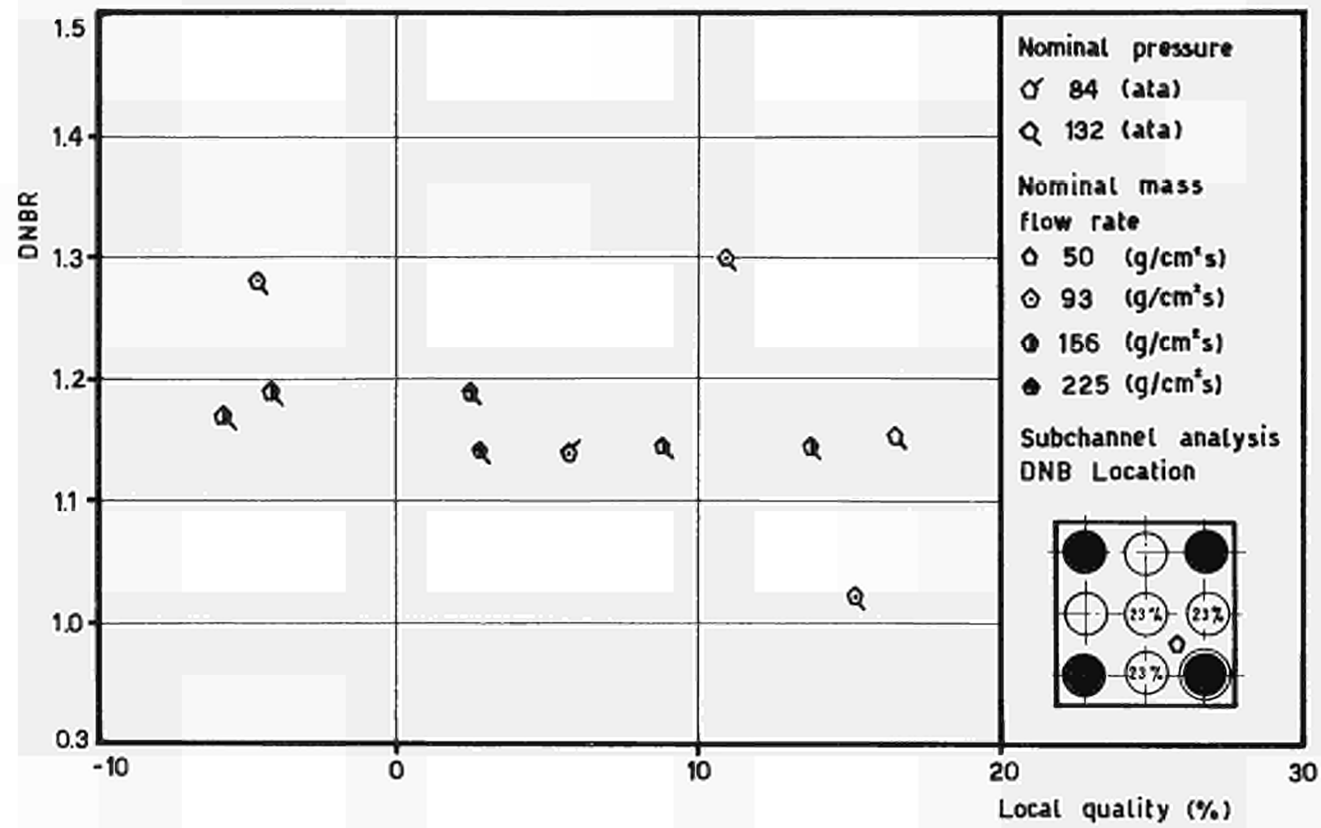

Fig. 14 - DNB Ratios according to W-3 correlation for channel B set II.4

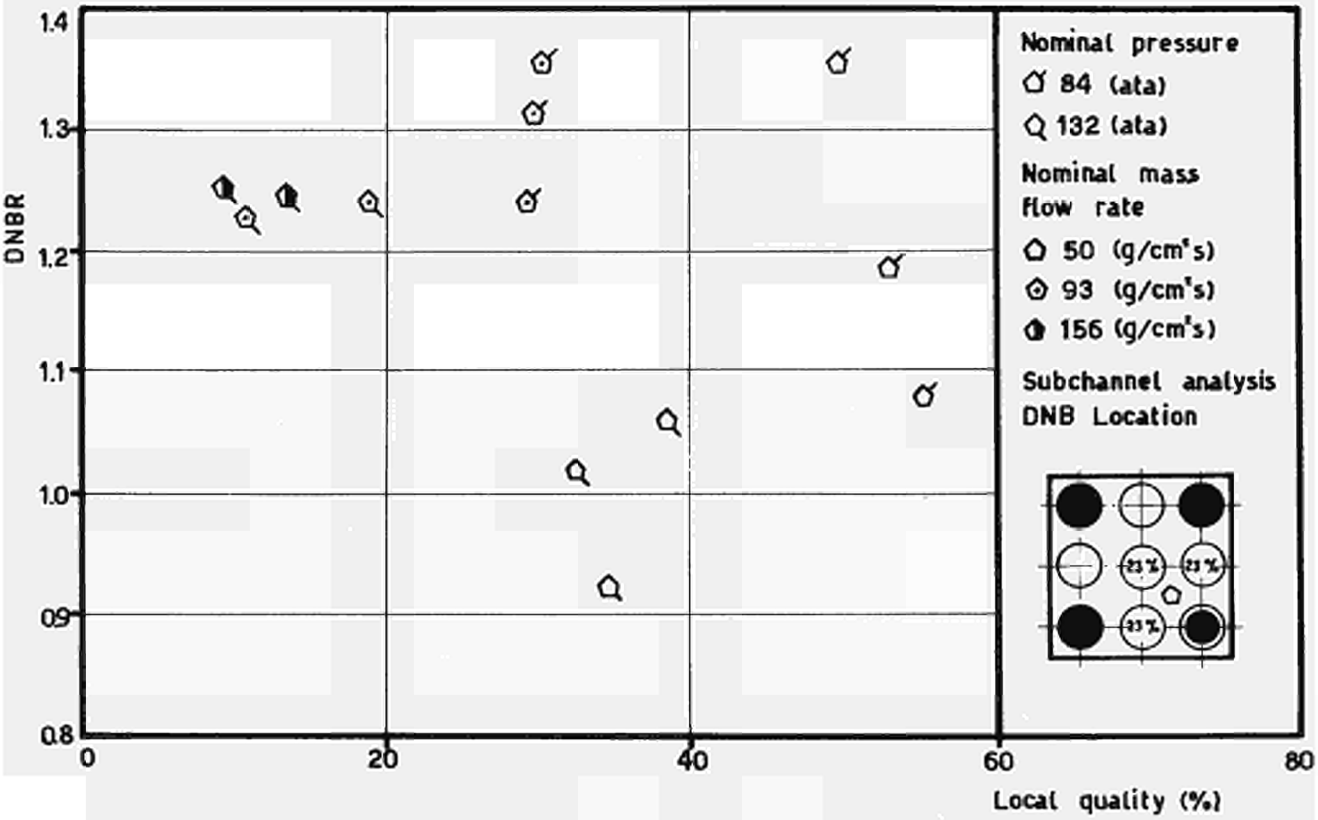

Fig. 15 - DNB Ratios according to ΔH-FIAT correlation for channel B set II.4

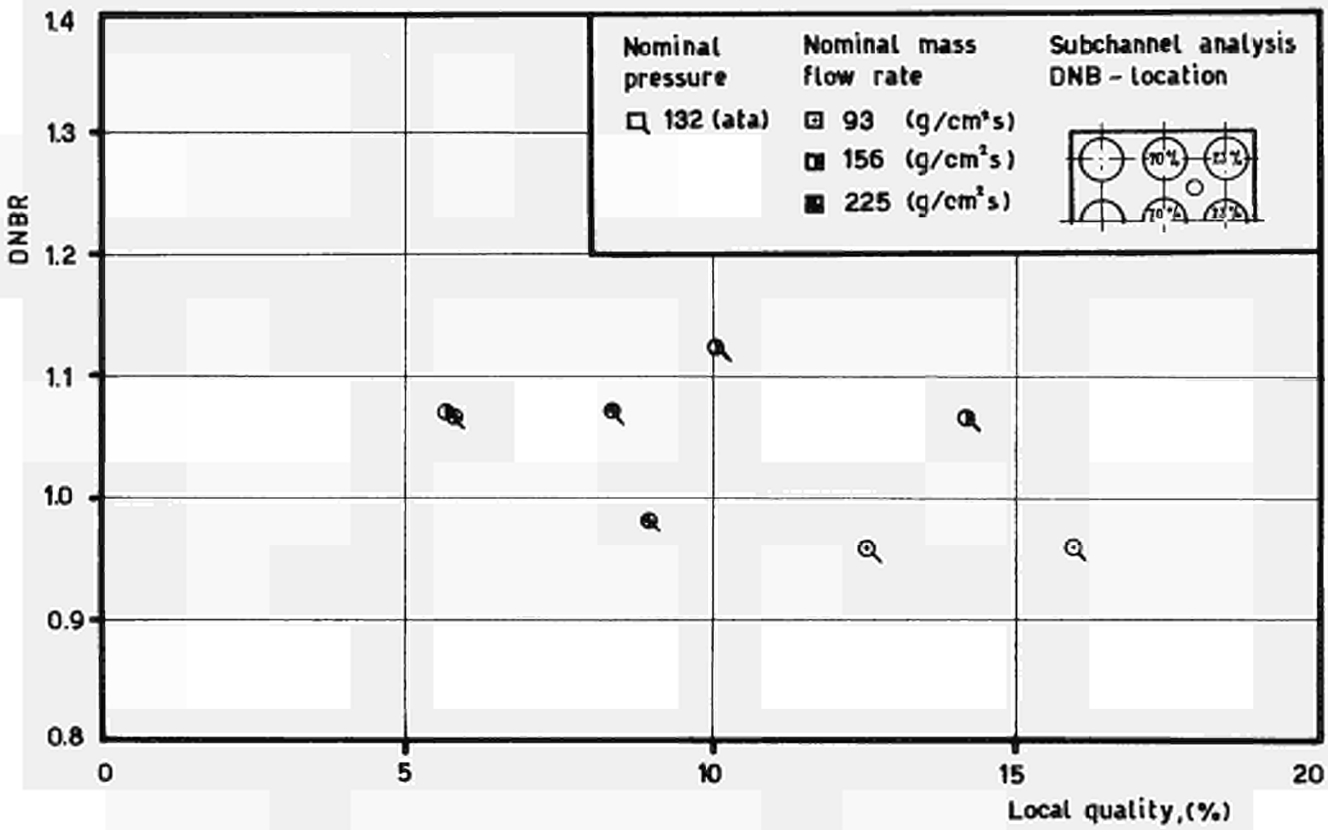

Fig. 16 - DNB Ratios according to W-3 correlation for channel B set II.5

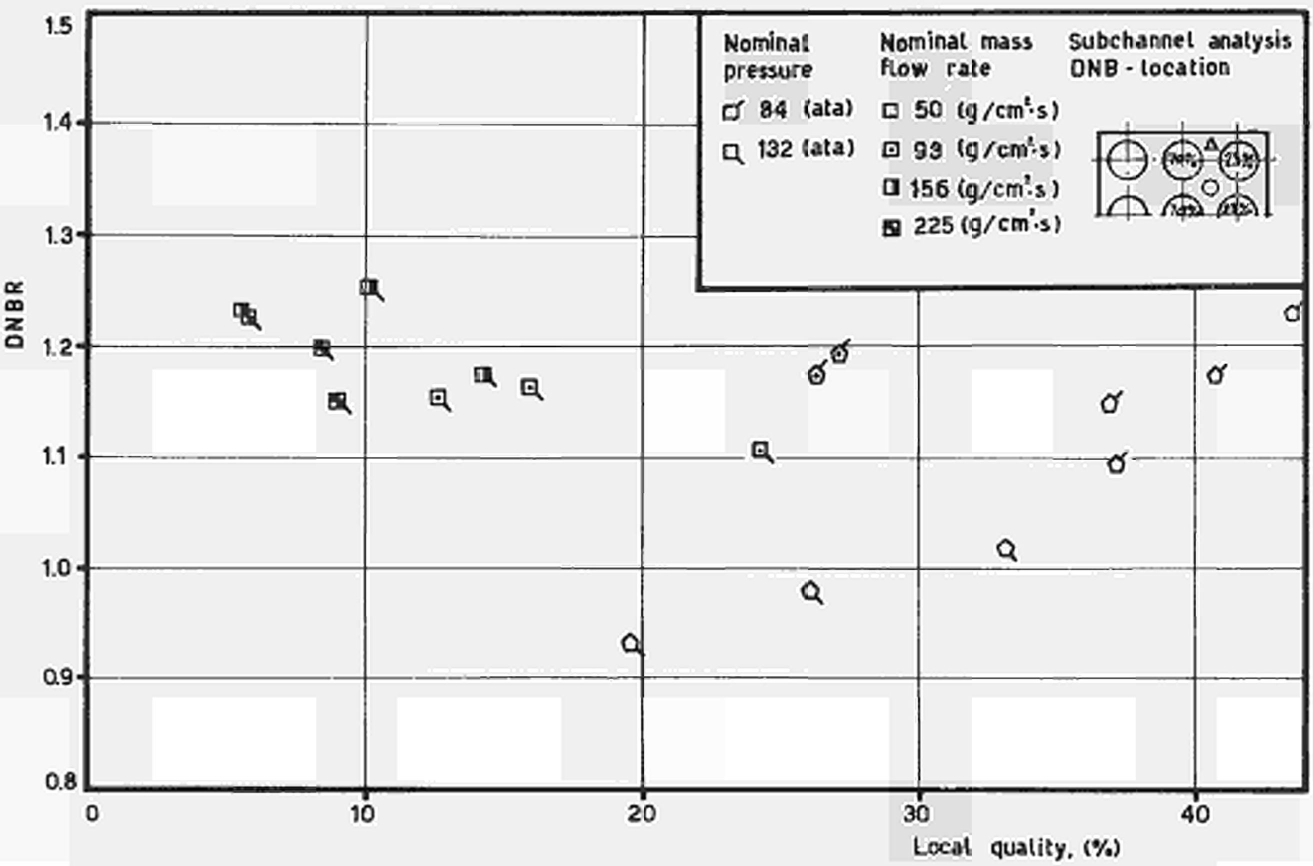

Fig. 17 - DNB Ratios according to ΔH-FIAT correlation for channel B set II.5

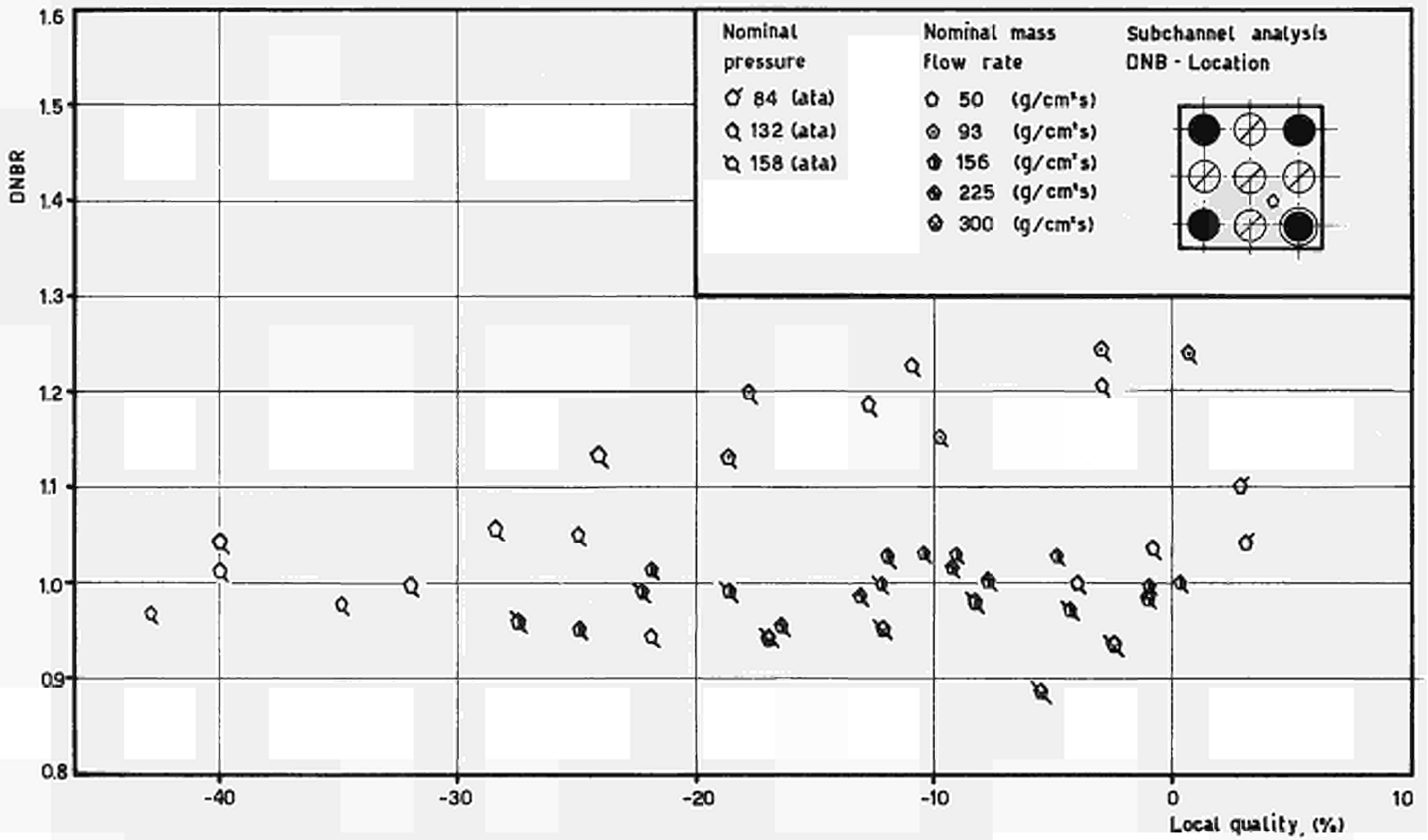

Fig. 18 – DNB Ratios according to W-3 correlation for channel B set III

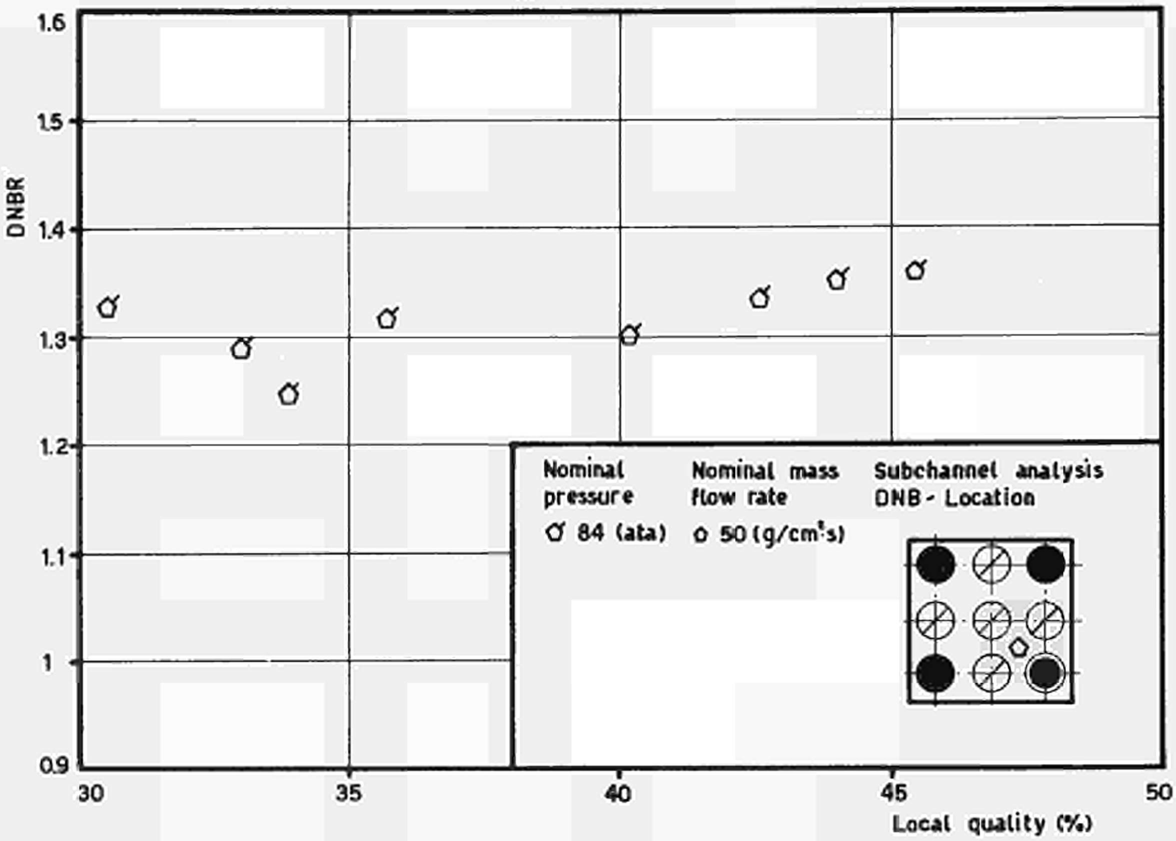

Fig. 19 - DNB Ratios according to △H-FIAT correlation for channel B set III

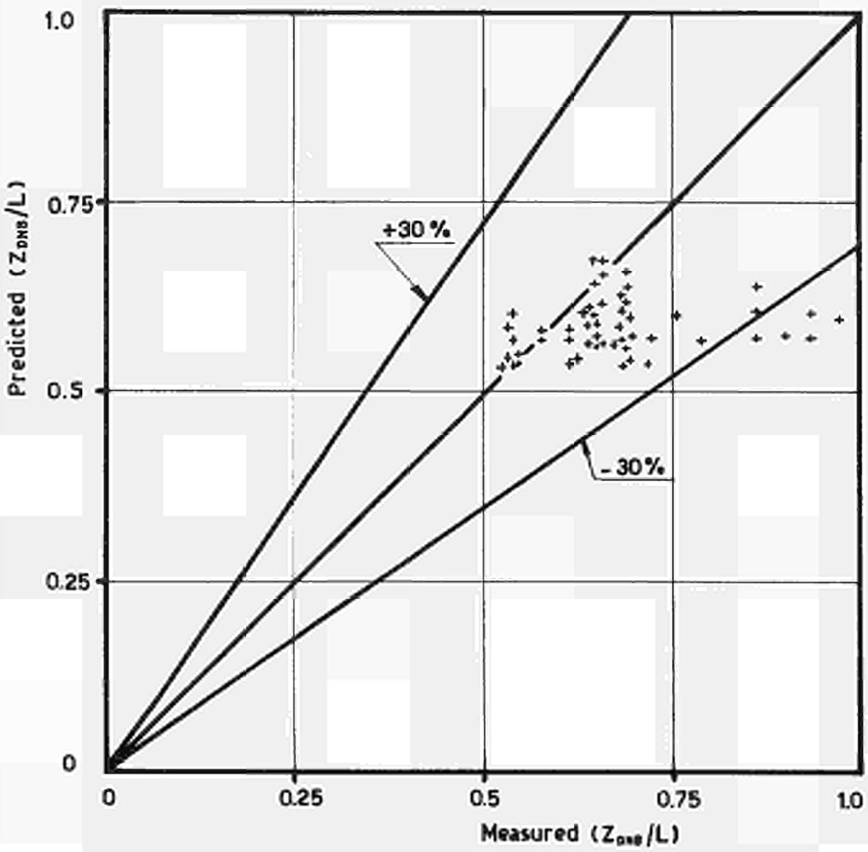

Fig. 20 - Comparison between predicted and measured (W-3 correlation) DNB position for axial non-uniform tests (ch. B set III)

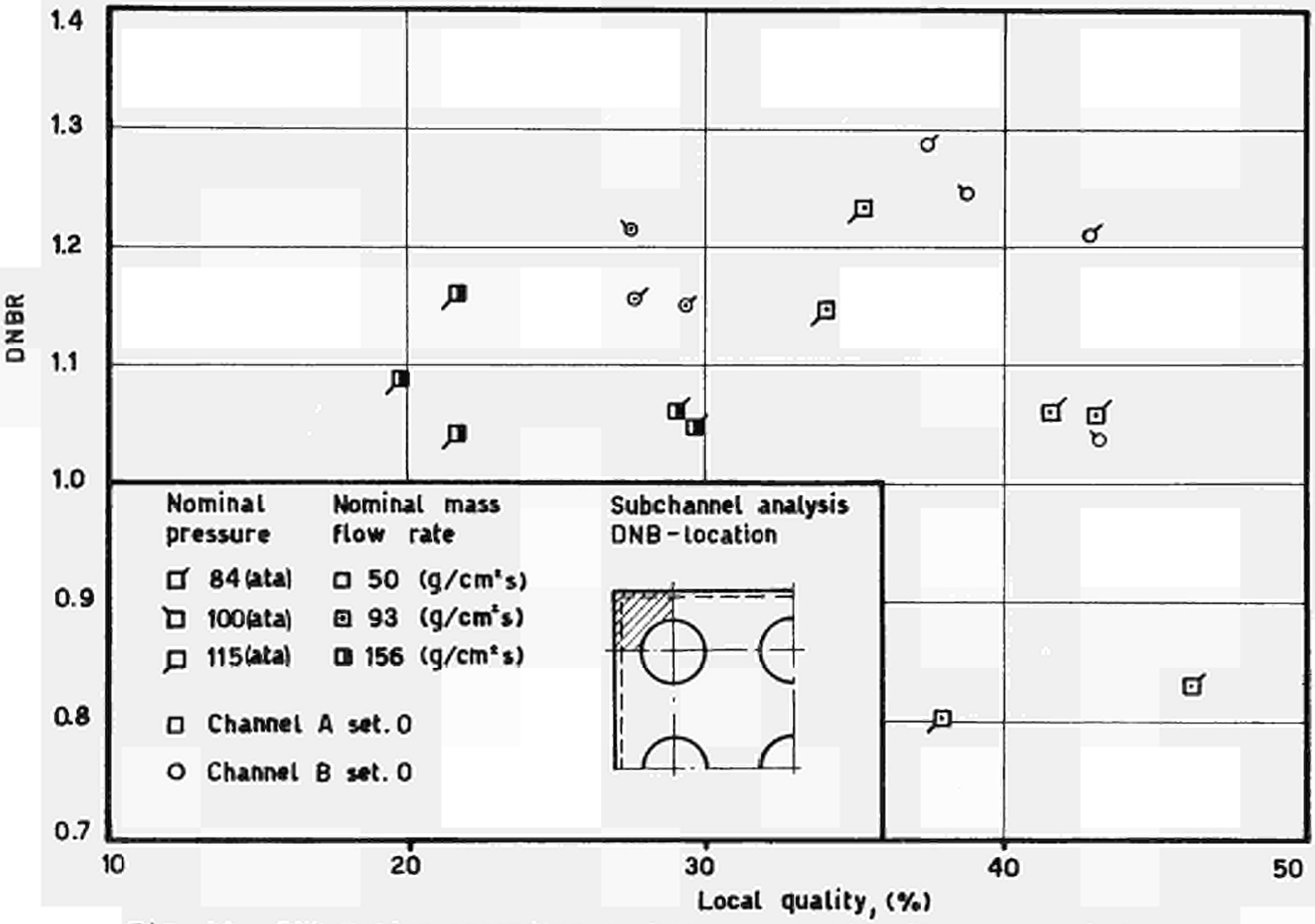

Fig. 21 - DNB Ratios according to G.E. correlation (Corner Cell) for channels A and B set O.

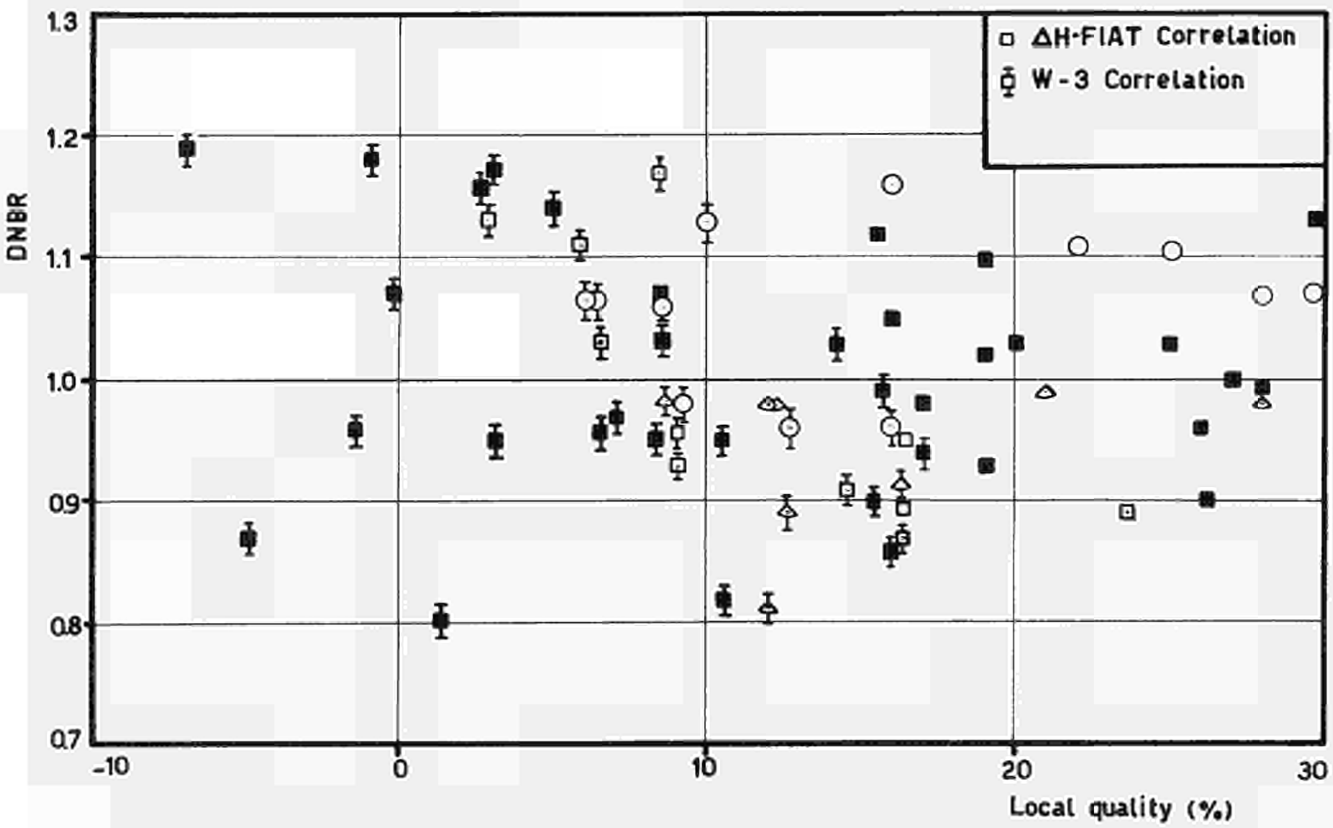

Fig. 22 - DNB Ratios according to ΔH-FIAT and W-3 correlations in subchannels without cold wall for various tests.

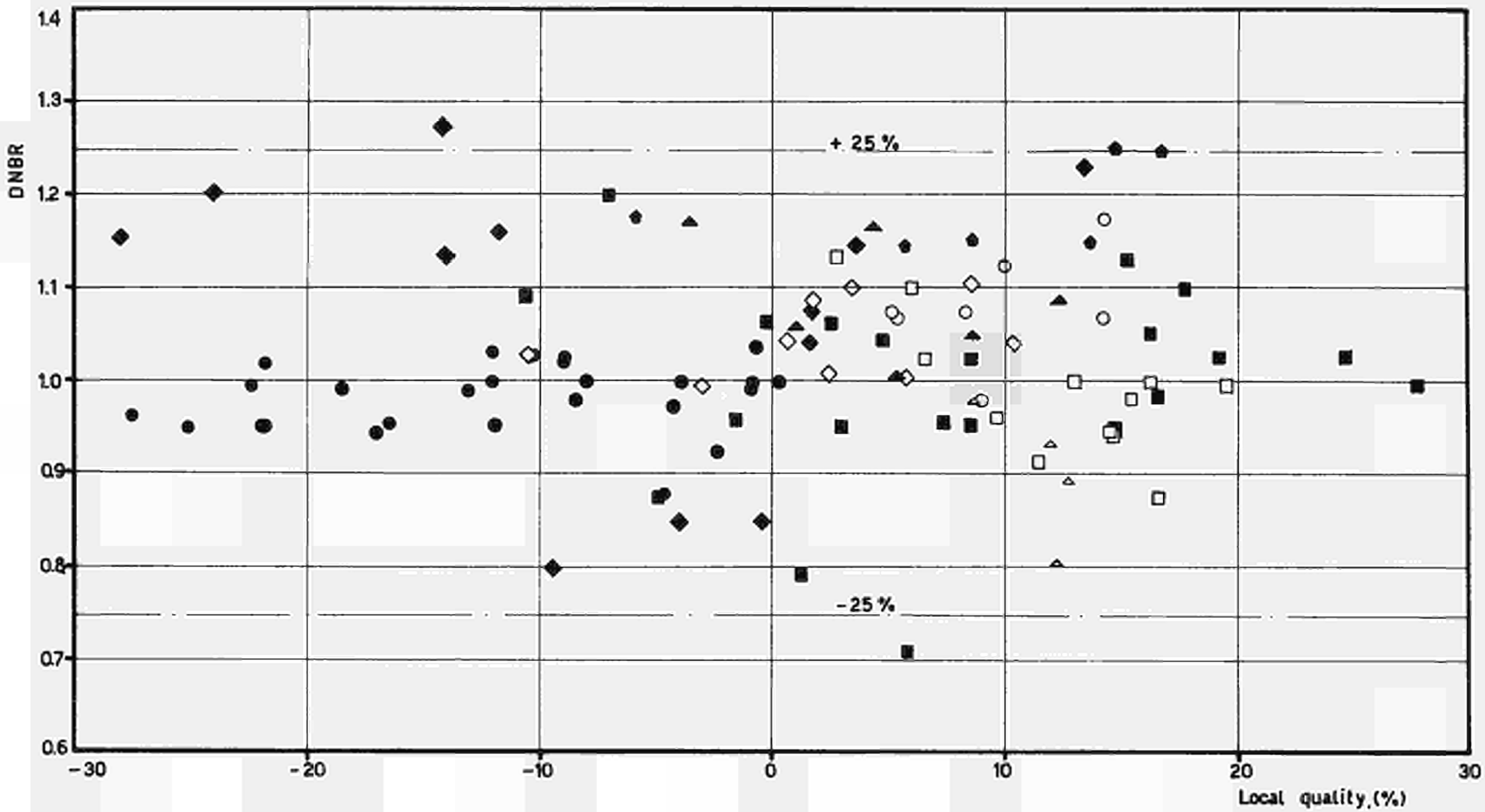

Fig. 23 - DNB Ratios in the range of complete validity of W-3 and ΔH-FIAT correlations for various tests.

NOTICE TO THE READER

All scientific and technical reports published by the Commission of the European Communities are announced in the monthly periodical **"euro-abstracts"**. For subscription (1 year: B.Fr. 1 025,—) or free specimen copies please write to:

Office for Official Publications
of the European Communities
Case postale 1003
Luxembourg 1
(Grand-Duchy of Luxembourg)

To disseminate knowledge is to disseminate prosperity — I mean general prosperity and not individual riches — and with prosperity disappears the greater part of the evil which is our heritage from darker times.

Alfred Nobel

SALES OFFICES

The Office for Official Publications sells all documents published by the Commission of the European Communities at the addresses listed below, at the price given on cover. When ordering, specify clearly the exact reference and the title of the document.

GREAT BRITAIN AND THE COMMONWEALTH

H.M. Stationery Office
P.O. Box 569
London S.E. 1

UNITED STATES OF AMERICA

European Community Information Service
2100 M Street, N.W.
Suite 707
Washington, D.C. 20 037

BELGIUM

Moniteur belge — Belgisch Staatsblad
Rue de Louvain 40-42 — Leuvenseweg 40-42
1000 Bruxelles — 1000 Brussel — Tel. 12 00 26
CCP 50-80 — Postgiro 50-80

Agency :
Librairie européenne — Europese Boekhandel
Rue de la Loi 244 — Wetstraat 244
1040 Bruxelles — 1040 Brussel

GRAND DUCHY OF LUXEMBOURG

Office for official publications of the European Communities
Case postale 1003 — Luxembourg 1
and 29, rue Aldringen, Library
Tel. 4 79 41 — CCP 191-90
Compte courant bancaire : BIL 8-109/6003/200

FRANCE

Service de vente en France des publications des Communautés européennes
26, rue Desaix
75 Paris-15e — Tel. (1) 306.5100
CCP Paris 23-96

GERMANY (FR)

Verlag Bundesanzeiger
5 Köln 1 — Postfach 108 006
Tel. (0221) 21 03 48
Telex : Anzeiger Bonn 08 882 595
Postscheckkonto 834 00 Köln

ITALY

Libreria dello Stato
Piazza G. Verdi 10
00198 Roma — Tel. (6) 85 09
CCP 1/2640

Agencies :
00187 Roma — Via del Tritone 61/A e 61/B
00187 Roma — Via XX Settembre (Palazzo Ministero delle finanze)
20121 Milano — Galleria Vittorio Emanuele 3
80121 Napoli — Via Chiaia 5
50129 Firenze — Via Cavour 46/R
16121 Genova — Via XII Ottobre 172
40125 Bologna — Strada Maggiore 23/A

NETHERLANDS

Staatsdrukkerij- en uitgeverijbedrijf
Christoffel Plantijnstraat
's-Gravenhage — Tel. (070) 81 45 11
Giro 425 300

IRELAND

Stationery Office
Beggar's Bush
Dublin 4

SWITZERLAND

Librairie Payot
6, rue Grenus
1211 Genève
CCP 12-236 Genève

SWEDEN

Librairie C.E. Fritze
2, Fredsgatan
Stockholm 16
Post Giro 193, Bank Giro 73/4015

SPAIN

Libreria Mundi-Prensa
Castello, 37
Madrid 1

OTHER COUNTRIES

Sales Office for official publications of the European Communities
Case postale 1003 — Luxembourg 1
Tel. 4 79 41 — CCP 191-90
Compte courant bancaire : BIL 8-109/6003/200

OFFICE FOR OFFICIAL PUBLICATIONS OF THE EUROPEAN COMMUNITIES
Case postale 1003 — Luxembourg 1
5921

CDNA04875ENC